J Neurosurg 102:470–475, 2005

Asymptomatic microbleeds in moyamoya disease: T_2*-weighted gradient-echo magnetic resonance imaging study

KEN-ICHIRO KIKUTA, M.D., PH.D., YASUSHI TAKAGI, M.D., PH.D., KAZUHIKO NOZAKI, M.D., PH.D., TAKASHI HANAKAWA, M.D., PH.D., TSUTOMU OKADA, M.D., NOBUHRO MIKUNI, M.D., PH.D., YUKIO MIKI, M.D., PH.D., YASUTAKA FUSHIMI, M.D., AKIRA YAMAMOTO, M.D., KEISUKE YAMADA, M.D., PH.D., HIDENAO FUKUYAMA, M.D., PH.D., AND NOBUO HASHIMOTO, M.D., PH.D.

Departments of Neurosurgery, Nuclear Medicine and Diagnostic Radiology, and Emergency Medicine, Kyoto University Graduate School of Medicine; Human Brain Research Center, Kyoto University School of Medicine, Kyoto, Japan

Object. The aim of this study was to investigate the incidence of asymptomatic microbleeds (MBs) in patients with moyamoya disease (MMD) by using a 3-tesla magnetic resonance (MR) imaging unit.

Methods. Data on 63 patients hospitalized with MMD between 1999 and 2004 were retrospectively examined to determine the incidence of asymptomatic MBs. Gradient-echo T_2*-weighted MR imaging studies obtained using 3- and 1.5-tesla units were available in 25 patients. These patients consisted of five men and 20 women, ranging in age from 17 to 66 years (mean age 41 ± 14 years). Ischemic MMD was diagnosed in 18 patients, and hemorrhagic MMD in seven. The incidence of MBs was also evaluated using the same 3-tesla MR imaging unit in 34 healthy volunteers including seven men and 27 women, ranging in age from 18 to 71 years (mean age 33 ± 12 years). Using the 3-tesla MR unit, asymptomatic MBs were demonstrated in 11 patients (44%); they were detected in seven patients (28%) by using the 1.5-tesla unit. In the 3-tesla MR studies in healthy individuals, MBs were found in two patients (5.8%). Based on 3-tesla MR studies, the incidence of MBs was significantly higher in patients with MMD compared with that in healthy individuals. Asymptomatic MBs were demonstrated in eight (44%) of 18 patients with ischemic MMD and three (43%) of seven patients with hemorrhagic MMD.

Conclusions. Microbleeds are significantly more common in patients with MMD than in healthy individuals regardless of the disease type. The evaluation of MBs with T_2*-weighted 3-tesla MR imaging might contribute to the treatment of MMD.

KEY WORDS • **moyamoya disease** • **microbleed** • **T_2*-weighted magnetic resonance imaging**

MOYAMOYA disease has been considered a progressive stenoocclusive disease at the terminal portion of bilateral internal carotid arteries, with moyamoya vessels developing as collateral channels.[4] This disease entity has been classified roughly into two types according to clinical features: ischemic MMD and hemorrhagic MMD. The former type is characterized by the onset of transient ischemic attack or cerebral infarction. In such cases, SPECT scanning usually reveals decreased rCBF. The latter type is distinguished by the onset of intracranial hemorrhage, which is usually confirmed on CT scanning.[4] Ischemic MMD usually occurs in pediatric patients, whereas almost half of the hemorrhagic MMD cases occur in adults.[4] Although surgical revascularization has been thought to be beneficial in patients with ischemic MMD, the efficacy of the procedure remains equivocal in patients with hemorrhagic MMD. Determining the type of MMD from which a patient suffers is crucial in the treatment of the disease.[12]

Gradient-echo T_2*-weighted MR imaging is extremely sensitive in detecting small remains of previously asymptomatic cerebral MBs.[6,15] Previous histopathological reports have shown that these small areas of signal loss are correlated with perivascular hemosiderin deposition around angiopathic arterioles.[3] Microbleeds are frequently detected in patients with lacunar infarction as well as in those with primary ICH and even in a small number of healthy individuals, usually in the corticosubcortical regions and the basal ganglia/thalami.[8,14] Microbleeds may be seen as general markers of various types of bleeding-prone cerebral microangiopathy or vascular vulnerability.[16] In this paper, we attempted to provide information pertaining to asymptomatic MBs in patients with MMD based on a retrospective analysis of MR imaging studies.

Abbreviations used in this paper: CT = computerized tomography; FLAIR = fluid-attenuated inversion-recovery; FOV = field of view; ^{123}I-IMP = iodine-123–labeled *N*-isopropyl-p-iodoamphetamine; ICH = intracerebral hemorrhage; MB = microbleed; MMD = moyamoya disease; MPRAGE = magnetization-prepared rapid acquisition gradient echo; MR = magnetic resonance; rCBF = regional cerebral blood flow; SPECT = single-photon emission CT.

Clinical Material and Methods

Patient Population

Between 1999 and 2004, 63 patients with MMD were ad-

mitted to our clinic. The MMD was diagnosed using cerebral angiography studies, according to the diagnostic criteria updated in 1997.[4] Based on clinical and radiological findings, 55 patients had a diagnosis of ischemic MMD, and eight hemorrhagic MMD. Routine radiological evaluation of MMD has been performed using CT and SPECT scanning and 1.5-tesla MR imaging without T_2*-weighted gradient-echo images. Eighty-four revascularization surgeries were performed in 57 patients between 1999 and 2004, and 23 surgeries were performed before 1999.

Since November 2003, T_2*-weighted gradient-echo images acquired using 3- and 1.5-tesla MR units were available in 25 patients who had been admitted to our clinic or were outpatients. These patients consisted of five men and 20 women, ranging in age from 17 to 66 years (mean age 41 ± 14 years). Ischemic MMD was diagnosed in 18 patients, and hemorrhagic MMD in seven. Among the 18 patients with ischemic MMD, three were men and 15 were women, with a mean age of 40 ± 14 years. Five of the 18 patients underwent the MR imaging studies before revascularization surgery, and the remaining 13 underwent imaging after revascularization. Five of these 13 patients experienced delayed symptomatic hemorrhage after surgery and before MR imaging. In the seven patients with hemorrhagic MMD, two were men and five were women, with a mean age of 40 ± 17 years. Four of these seven patients underwent MR imaging before surgery and three after surgery. No patients among those with hemorrhagic MMD experienced recurrent hemorrhage either before or after surgery. In total, nine patients underwent MR imaging before revascularization and 16 patients underwent imaging after surgery (Table 1).

Among the 25 patients, 11 were receiving antiplatelet drug therapy at the time of MR imaging. Six patients had never received antiplatelet therapy and the remaining eight patients each had a history of antiplatelet therapy but had discontinued it more than 1 year before MR imaging. Patients with cerebral aneurysms confirmed on angiography were excluded from this study, and no patient was studied within 24 hours after angiography.

The incidence of MBs in 34 healthy volunteers was also studied using the same 3-tesla MR unit. These seven men and 27 women ranged in age from 18 to 71 years (mean age 33 ± 12 years; Table 2).

TABLE 1

Summary of characteristics in 25 patients with MMD

Variable	Ischemic MMD	Hemorrhagic MMD	MMD
total no. of patients	18	7	25
male/female ratio	3:5	2:5	5:20
mean age (yrs)*	40 ± 14	40 ± 17	41 ± 14
patients w/ MBs	8	3	11
MRI before surgery			
no. of patients	5	4	9
no. w/ MBs	3	2	5
no. w/ postop symptomatic hemorrhage	0	0	0
no. w/ MBs	0	0	0
MRI after surgery			
no. of patients	13	3	16
no. w/ MBs	5	1	6
no. w/ postop symptomatic hemorrhage	5	0	5
no. w/ MBs	3	0	3

* Values represent the means ± standard deviations.

Magnetic Resonance Images

All patients underwent imaging studies with the same 3-tesla MR unit (Magnetom Trio; Siemens, Enlargen, Germany). Axial T_2*-weighted gradient-echo sequences were obtained (TR 612 msec; TE 18 msec; flip angle 20°; matrix 256 × 224; FOV 22 cm; slices 19; slice thickness 5 mm; and interslice gap 1.5 mm). At the same time, axial T_2-weighted turbo–spin echo sequences (TR 8400 msec; TE 108 msec; flip angle 150°; matrix 512 × 448; FOV 22 cm; slices 40; slice thickness 2.3 mm; and interslice gap 0.7 mm) and axial T_1-weighted three-dimensional MPRAGE sequences (TR 2000 msec; TE 4.4 msec; TI 990 msec; flip angle 8°; matrix 256 × 224; FOV 24 cm; slices 208; and slice thickness 1 mm) were acquired to distinguish MBs from the signal voids of cerebral arteries and from other mass lesions with hemorrhage such as cavernous angiomas.

During the 1.5-tesla MR imaging study, axial T_2*-weighted gradient-echo sequences (TR 700 msec; TE 17 msec; flip angle 20°; matrix 256 × 168; section thickness 5 mm; and interslice gap 1 mm) were obtained using the same MR unit (Magnetom Symphony; Siemens). All images were reviewed by a single investigator (K.K.). Hypointense lesions representing MBs on the T_2*-weighted images were defined as small hypointense areas (< 10 mm in diameter) with well-defined margins.[3]

Asymptomatic MBs in patients with hemorrhagic MMD were defined as hypointense lesions demonstrated in the region separate from where hemorrhages existed on CT scanning at hemorrhagic onset.

Statistical Analysis

Data on the incidence of MBs were statistically evaluated using the chi-square test or the Fisher exact test. Differences were defined as significant at a probability level less than 0.05.

Results

Incidence of MBs on 3-Tesla Imaging Studies

Among the 25 patients with MMD, asymptomatic MBs were found in 11 (44%), that is, in eight (44%) of 18 patients with ischemic MMD and three (43%) of seven patients with hemorrhagic MMD. No significant difference was observed in the incidence of MBs between the two groups according to statistical analysis with the chi-square test ($p = 0.94$). Asymptomatic MBs were demonstrated in five (56%) of the nine patients who had undergone MR imaging before revascularization surgery and in six (38%) of the 16 patients who had undergone imaging after surgery (Table 1). In the 18 patients with ischemic MMD, 13 underwent MR imaging after revascularization. Five of these 13 patients experienced delayed symptomatic hemorrhage following surgery. Among patients with ischemic MMD, it was calculated that three (60%) of the five patients with postoperative delayed hemorrhage had asymptomatic MBs and two (25%) of the eight patients without had asymptomatic MBs. In the patients with hemorrhagic MMD, asymptomatic MBs occurred in two of four patients who had un-

TABLE 2

Incidence of MBs in 25 patients with MMD

Group	Total No. of Patients	Mean Age (yrs)	Male/Female Ratio	No. of Patients w/ MBs	Incidence of MBs (%)
patients w/ MMD who underwent 3-tesla MRI	25	41 ± 15	5:20	11	44
patients w/ MMD who underwent 1.5-tesla MRI	25	41 ± 15	5:20	7	28
healthy individuals who underwent 3-tesla MRI	34	33 ± 12	7:27	2	5.8

dergone imaging before surgery and in one of three patients who had undergone imaging after surgery.

As for the number of asymptomatic MBs, one was found in six patients, two in three patients, and three or more in two patients. Microbleeds were predominantly located in the periventricular white matter (Cases 5 and 7–11). Magnetic resonance images demonstrating MBs and information about the 11 patients with these lesions are shown in Fig. 1.

Asymptomatic MBs were detected in five (45%) of the 11 patients on antiplatelet therapy, three (33%) of the six patients with no history of antiplatelet therapy, and four (50%) of the eight patients with a history of antiplatelet therapy. There was no significant difference in the incidence of MBs among these three groups according to statistical analysis with the chi-square test.

Illustrative Case: Case 5

This 49-year-old man presenting with recurrent transient attacks of left hemiparesis and left hemiparesthesia was admitted to our clinic in April 2004. An ^{123}I-IMP SPECT study revealed decreased rCBF in the bilateral frontal lobes (Fig. 2A). Results of FLAIR imaging with a 1.5-tesla MR unit demonstrated ischemic lesions in the deep white matter of the bilateral frontal lobes (Fig. 2B). No hemorrhagic lesion was revealed on CT scanning (Fig. 2C). According to the clinical symptoms and routine radiological studies, ischemic MMD was diagnosed. Nonetheless, T_2*-weighted imaging with a 3-tesla MR unit clearly revealed multiple MBs in the periventricular regions (Fig. 2D).

Incidence of MBs in Healthy Individuals

Asymptomatic MBs were demonstrated in two (5.8%) of 34 healthy volunteers examined using a 3-tesla MR unit (Table 2). One volunteer was a 55-year-old woman with an asymptomatic MB in the right caudoputamen. The other volunteer was a 26-year-old woman with an MB in the right occipital lobe. In the latter case the lesion was demonstrat-

Case	1	2	3	4	5	6	7	8	9	10	11
Age	41	65	27	36	49	24	63	28	44	35	53
Sex	F	M	F	F	M	F	F	F	F	F	F
Diagnosis	ischemic MMD	ischemic MMD	ischemic MMD	ischemic MMD	ischemic MMD	ischemic MMD →op.→ hemorrhage	ischemic MMD →op.→ hemorrhage	ischemic MMD →op.→ hemorrhage	hemorrhagic MMD	hemorrhagic MMD	hemorrhagic MMD
Clinical course	2001/12 infarct	1945- TIA	2003/11TIA	1999/10 TIA	2003/11 infarct	1987 TIA 2003/10 hemorrhage	1981infarct 1985hemorrhage 1987 hemorrhage 1999 hemorrhage	1981 TIA 1998 hemorrhage	2000/8 hemorrhage	1999/11 hemorrhage	1979/11 hemorrhage
Date of op.	2002/9 lt. STA-MCA+EMS 2003/1 rt. STA-MCA+EMS	-	-	2000/3 rt. STA-MCA+EMS 2000/11 lt. STA-MCA +EMS	-	1987 bilat. EDAS	1987 bilat. STA-MCA+EMS	1982 bilat. STA-MCA+EMS	-	2002/8 lt. STA-MCA 2002/10 rt. STA-MCA	1981/4 lt. STA-MCA
Timing of MRI study	postop. 2003/11	preop. 2003/11	preop. 2003/12	postop. 2004/3	preop. 2004/4	postop. 2003/10	postop. 2004/3	postop. 2004/2	preop. 2003/11	postop. 2004/3	postop. 2004/3
MRI demonstrating silent MBs	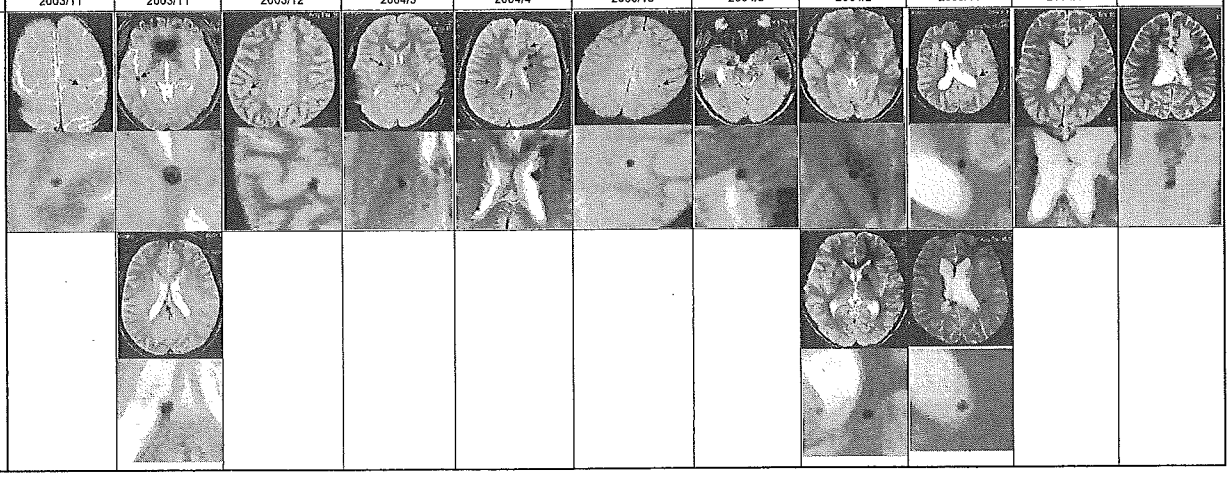										

FIG. 1. Chart demonstrating patient age and sex, disease diagnosis, clinical course, dates of surgery and MR imaging studies, and T_2*-weighted gradient-echo images, obtained using the 3-tesla unit in the 11 patients, revealing hypointense dot spots. Magnified versions of the T_2*-weighted images are featured below each original image. EDAS = encephaloduroarterio synangiosis; EMS = encephalomyosynangiosis; STA–MCA = superficial temporal artery–middle cerebral artery; — = not applicable.

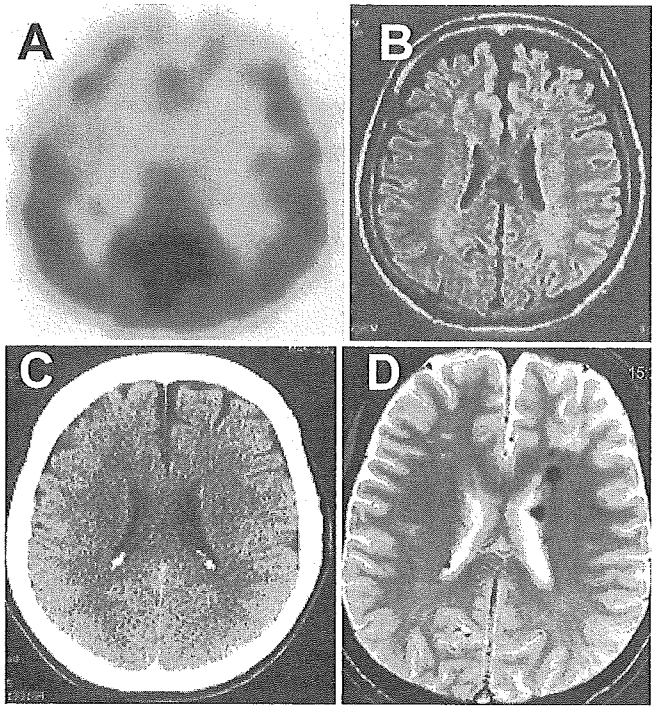

FIG. 2. Case 5. A: An ^{123}I-IMP SPECT scan revealing decreased rCBF in the bilateral frontal lobes. B: A FLAIR 1.5-tesla MR image demonstrating mild ischemic lesions in the deep white matter of the frontal lobes. C: A CT scan displaying no hemorrhagic lesion. D: A T_2*-weighted 3-tesla MR image revealing multiple MBs in the periventricular regions.

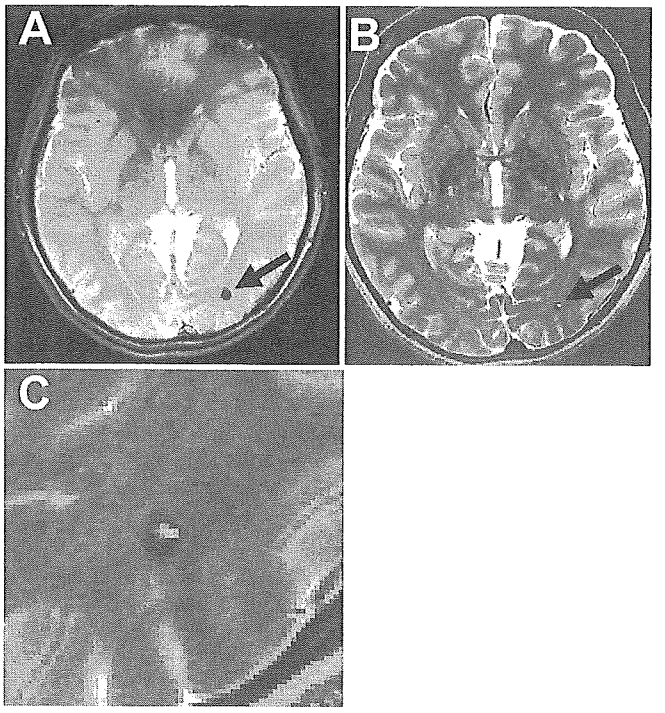

FIG. 3. A T_2*-weighted 3-tesla image (A) and T_2-weighted images (B and C) obtained in a 26-year-old healthy female volunteer. The former image demonstrates an MB *(arrow)* in the right occipital lobe, which was described as a heterogeneous intensity mass on T_2-weighted imaging, indicating that the lesion can be diagnosed as cavernous angioma. Note that C is a magnified version of the image in B.

ed as a heterogeneous mass on MPRAGE imaging and was diagnosed as incidental cavernous angioma (Fig. 3A and B). The incidence of MBs in the 3-tesla MR study was significantly higher in the patients with MMD than in healthy individuals ($p = 0.0005$, chi-square test).

Comparison of Sensitivity in Detecting MBs Between 3- and 1.5-Tesla MR Units

Whereas asymptomatic MBs were found in 11 (44%) of 25 patients in the 3-tesla study, these lesions could be detected in only seven (28%) of 25 patients in the 1.5-tesla study (Table 2). The quality of the images obtained using the 3-tesla unit was greater than that of the images acquired with the 1.5-tesla unit. For example, an asymptomatic MB was demonstrated clearly on the 3-tesla study in Cases 3 and 8 but not on the 1.5-tesla study (Fig. 4). Nonetheless, there was no statistically significant difference in sensitivity between the two MR units in this study ($p = 0.239$, chi-square test).

Discussion

Effectiveness of the 3-Tesla MR Unit in Detecting Asymptomatic MBs in Patients With MMD

Cerebral MBs were detected using gradient-echo T_2*-weighted MR imaging in 51 to 80% of patients with primary ICH,[10,14] in 20 to 36% of patients with ischemic stroke,[2,8,13] in 32% of patients with Alzheimer disease,[5] and in 31 to 69% of patients with cerebral autosomal-dominant arteriopathy with subcortical infarcts and leukoencephalopathy;[1,11] they were detected in 6.4 to 9.8% of healthy individuals.[8,15,16] Therefore, MBs can be thought of as general markers of various types of bleeding-prone cerebral angiopathy.[16]

In the 3-tesla MR study, the incidence of asymptomatic MBs in patients with MMD, with ischemic MMD, and with hemorrhagic MMD was 44, 44, and 43%, respectively. There was no significant difference in the incidence of MBs between the two MMD onset types. As for the incidence in healthy individuals in the 3-tesla study, MBs were found in only 5.8%, a rate not so different from the MB incidence in healthy individuals in previous 1.5-tesla studies.[8,15,16] The incidence of asymptomatic MBs in patients in the 3-tesla study was significantly higher than that in healthy individuals regardless of the MMD onset type.

Data from previous autopsy studies have revealed that ruptured or dilated vessels with diminution of the elastic lamina, stenotic vessels with wall thickening, and vessels along with microaneurysm formation could be observed simultaneously in a patient with MMD.[18] Our data indicate that ischemic and hemorrhagic lesions can coexist in the same patient with MMD. These findings might suggest that MB occurs with equal probability regardless of the MMD onset type.

Microbleeds were observed predominantly in the periventricular deep white matter in patients with MMD, al-

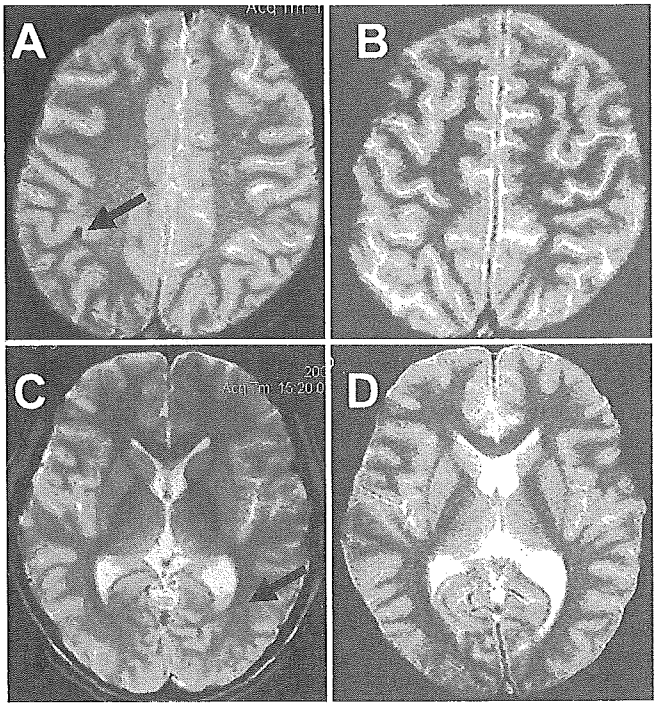

FIG. 4. Case 3. A T_2*-weighted image (A) obtained with a 3-tesla MR unit, demonstrating an MB in the white matter of the right parietal lobe, which was not revealed on an image (B) obtained using the 1.5-tesla unit. Case 8. A T_2*-weighted image (C) obtained with a 3-tesla MR unit, revealing an MB in the left occipital lobe, which could not be detected on an image (D) obtained using the 1.5-tesla unit.

though they were usually found in corticosubcortical regions or the basal ganglia/thalami in patients with other pathological conditions.[8,14] These observations are compatible with the fact that intraventricular hemorrhage is common in patients with hemorrhagic MMD associated with an increased hemodynamic load in the vessels supplying the walls of the ventricles or periventricular region, as previously reported.[7]

Although most data in previous reports were obtained using 1.5-tesla MR units,[1,2,5,8,10,11,13–16] we used a 3-tesla unit in the present study because images acquired with the higher-field MR imaging unit seem to have better resolution than those obtained with the lower field. Nonetheless, a comparison study in this small series could not reveal a significant difference in the sensitivity in detecting MBs between the two MR units.

Wong, et al.,[17] reported that MBs were found more frequently in aspirin users with a history of ICH. At our institution, antiplatelet therapy is routinely indicated in patients with ischemic MMD until 6 to 12 months after revascularization surgery but not in patients with hemorrhagic MMD. Therefore, our series included at the time of MR imaging 11 patients on antiplatelet therapy, six with no history of antiplatelet therapy, and eight with a history of antiplatelet therapy. Although the incidence of MBs was relatively higher in patients currently on or with a history of antiplatelet therapy compared with patients with no history, there was no significant difference.

Relationship Between the Incidence of MBs and Revascularization Surgery, and MBs as Potential Predictors of Subsequent Postoperative Hemorrhage in MMD

Data in recent reports have revealed that the existence of MBs appears to be a potential risk factor for subsequent intracranial hemorrhage following ischemic stroke[2,12] or for major symptomatic hemorrhage following intraarterial thrombolytic therapy.[9] Fan, et al.,[2] conducted a prospective analysis of 121 patients with acute cerebral infarction and reported that four (9.3%) of 43 patients with MBs had ICH during the follow-up period of 27 months.

In our study, asymptomatic MBs were found in 56% of the patients who underwent MR imaging before revascularization surgery and in 38% of the patients who underwent imaging after surgery. Because it is unclear when MBs occurred in our series, the effects of revascularization surgery on the occurrence of MBs could not be evaluated. In the patients with ischemic MMD, MBs were found in 60% of the patients with delayed hemorrhage after surgery and in 25% of the patients without. Although these observations might indicate that MBs are a potential risk factor for hemorrhage following revascularization surgery in patients with ischemic MMD, a large cohort study is required to resolve this issue.

Given that there was no patient with hemorrhagic MMD who had experienced recurrent hemorrhage before MR imaging, the relationship between the presence of MBs and the probability of recurrent hemorrhage in patients with hemorrhagic MMD could not be evaluated. Currently, a cohort, randomized, controlled study of MMD in adults in Japan (JAM trial) is in progress to determine whether superficial temporal artery–middle cerebral artery anastomosis has prophylactic effects against recurrent hemorrhages in patients with hemorrhagic MMD.[11] The evaluation of MBs combined with the aforementioned study would provide useful information on this issue.

Conclusions

Our data provide the first evidence that MBs can be found significantly more often in patients with MMD than in healthy individuals, regardless of the reason for MMD onset. Evaluation of MBs by using T_2*-weighted 3-tesla MR imaging might contribute to the treatment of MMD.

Acknowledgment

We gratefully acknowledge the kind cooperation of the personnel in the neurosurgical and radiological departments at Kyoto University Hospital in obtaining the data for the volunteer MR imaging study.

References

1. Dichgans M, Holtmannspotter M, Herzog J, Peters N, Bergmann M, Yousry TA: Cerebral microbleeds in CADASIL: A gradient-echo magnetic resonance imaging and autopsy study. **Stroke 33:** 67–71, 2002
2. Fan YH, Zhang L, Lam WWM, Mok VCT, Wong KS: Cerebral microbleeds as a risk factor subsequent intracerebral hemorrhages among patients with acute ischemic stroke. **Stroke 34:** 2459–2462, 2003

3. Fazekas F, Kleinert R, Roob G, Kleinert G, Kapeller P, Schmidt R, et al: Histopathologic analysis of foci of signal loss on gradient-echo T2*-weighted MR images in patients with spontaneous intracerebral hemorrhages: evidence of microangiopathy-related microbleeds. **AJNR 20:**637–642, 1999
4. Fukui M: Guidelines of the diagnosis and treatment of spontaneous occlusion of the circle of Willis ('moyamoya' disease). Research Committee On Spontaneous Occlusion of the Circle of Willis (Moyamoya Disease) of the Ministry of Health and Welfare, Japan. **Clin Neurol Neurosurg 99 (Suppl 2):**S238–S240, 1997
5. Hanyu H, Tanaka Y, Shimizu S, Takasaki M, Abe K: Cerebral microbleeds in Alzheimer's disease. **J Neurol 250:**1496–1497, 2003
6. Imaizumi T, Chiba M, Honma T, Niwa J: Detection of hemosiderin deposition by T2*-weighted MRI after subaracnoid hemorrhage. **Stroke 34:**1693–1698, 2003
7. Irikura K, Miyasaka Y, Kurata A, Tanaka R, Fujii K, Yada K, et al: A source of haemorrhage in adult patients with moyamoya disease: the significance of tributaries from the choroidal artery. **Acta Neurochir 138:**1282–1286, 1996
8. Kato H, Izumiyama M, Izumiyama K, Takahashi A, Itoyama Y: Silent cerebral microbleeds on T2*-weighted MR: correlation with stroketype, stroke recurrence, and leukoaraiosis. **Stroke 33:** 1536–1540, 2002
9. Kidwell CS, Saver JL, Villablanca JP, Duckwiler G, Fredieu A, Gough K, et al: Magnetic resonance imaging detection of microbleeds before thrombolysis: an emerging application. **Stroke 33:** 95–98, 2002
10. Lee SH, Bae HJ, Kwon SJ, Kim H, Kim YH, Yoon BW, et al: Cerebral microbleeds are regionally associated with intracerebral hemorrhage. **Neurology 62:**72–76, 2004
11. Lesnik Oberstein SAJ, van den Boom R, van Buchem MA, von Houwelingen HC, Bakker E, Vollebregt E, et al: Cerebral microbleeds in CADASIL. **Neurology 57:**1066–1070, 2001
12. Miyamoto S, Japan Adult Moyamoya Trial Group: Study design for a prospective randomized trial of extracranial-intracranial bypass surgery for adults with moyamoya disease and hemorrhagic onset—the Japan Adult Moyamoya Trial Group. **Neurol Med Chir 44:**218–219, 2004
13. Nighoghossian N, Hermier M, Adeleine P, Blanc-Lasserre K, Derex L, Honnorat J, et al: Old microbleeds are a potential risk factor for cerebral bleeding after ischemic stroke: a gradient-echo T2*-weighted brain MRI study. **Stroke 33:**735–742, 2002
14. Roob G, Lechner A, Schmidt R, Flooh E, Hartung HP, Fazekas F: Frequency and location of microbleeds in patients with primary intracerebral hemorrhage. **Stroke 31:**2665–2669, 2000
15. Roob G, Schmidt R, Kapeller P, Lechner A, Hartung HP, Fazekas F: MRI evidence of past cerebral microbleeds in a healthy elderly population. **Neurology 52:**991–994, 1999
16. Tsushima Y, Aoki J, Endo K: Brain microhemorrhages detected on T2*-weighted gradient-echo MR images. **AJNR 24:**88–96, 2003
17. Wong KS, Chan YL, Liu JY, Gao S, Lam WWM: Asymptomatic microbleeds as a risk factor for aspirin-associated intracerebral hemorrhages. **Neurology 60:**511–513, 2003
18. Yamashita M, Oka K, Tanaka K: Histopathology of the brain vascular network in moyamoya disease. **Stroke 14:**50–58, 1983

Manuscript received May 21, 2004.
Accepted in final form October 25, 2004.
Address reprint requests to: Ken-ichiro Kikuta, M.D., Ph.D., Department of Neurosurgery, Kyoto University Graduate School of Medicine, 54 Kawaharacho, Shogoin, Sakyo-ku, Kyoto 606-8507, Japan. email: kikuta@kuhp.kyoto-u.ac.jp.

Available online at www.sciencedirect.com

SCIENCE DIRECT®

Surgical Neurology 63 (2005) 480–484

SURGICAL NEUROLOGY

www.surgicalneurology-online.com

Vascular

An adult case of moyamoya syndrome that developed dural sinus thrombosis associated with protein C deficiency: case report and literature review

Ken-ichiro Kikuta, MD, PhD[a,*], Susumu Miyamoto, MD, PhD[a,b], Hiroharu Kataoka, MD, PhD[a], Keisuke Yamada, MD, PhD[a], Yasushi Takagi, MD, PhD[a], Kazuhiko Nozaki, MD, PhD[a], Nobuo Hashimoto, MD, PhD[a]

[a]*Department of Neurosurgery, Kyoto University Graduate School of Medicine, Shogoin, Sakyo-ku, Kyoto 606-8507, Japan*
[b]*Department of Neurovascular Surgery, National Cardiovascular Center, Suita, Osaka 565-8565, Japan*

Received 23 March 2004; accepted 27 April 2004

Abstract We describe a 54-year-old woman exhibiting MMS who developed delayed dural sinus thrombosis associated with PCD. Angiographic findings of the patient were so unusual that bilateral internal carotid arteries were occluded between their origin and the carotid fork with extensive development of collateral circulation via the external carotid arteries and the posterior cerebral arteries instead of moyamoya vessels at the base of the brain. Seven years after bilateral cerebral revascularization surgery, intracerebral hemorrhage occurred caused by dural sinus thrombosis. In the treatment for the patient with MMS associated with PCD, risk of sinus thrombosis should be taken into account.

Keywords: Moyamoya disease; Moyamoya syndrome; Protein C deficiency; Dural sinus thrombosis

1. Introduction

MMD has been considered a progressive steno-occlusive disease at the terminal portions of the bilateral internal carotid arteries (ICAs) with the development of moyamoya vessels as collateral channels [4]. Although the etiology of MMD remains unknown, similar angiographic findings are often observed in patients with several underlying diseases, which were defined as moyamoya syndrome (MMS) [4,7,11]. Moyamoya syndrome associated with PCD is rare and only 6 pediatric cases have been reported. We describe a 54-year-old woman exhibiting MMS associated with PCD that developed delayed dural sinus thrombosis. Pitfalls in the treatment for such patients are to be discussed with literature review.

2. Case report

The subject, a 54-year-old woman, suddenly developed right-sided hemiparesis and loss of consciousness on October 30, 1993, when she was 45 years old. Brain CT revealed an ischemic lesion in the left thalamus. Gradual but complete remission of her symptoms was obtained by conservative treatment. Cerebral angiography disclosed bilateral occlusion of the ICAs at their origin (Fig. 1B). Collateral circulation was developed via transdural anastomosis from the bilateral ECAs and via leptomeningeal anastomosis from the PCAs. Abnormal vasculature was observed mainly around the bilateral P2 portion of the PCA, and development of moyamoya vessels at the base of the brain was minimal (Fig. 1C-F). Bilateral carotid forks were

Abbreviations: CT, computed (axial) tomography; ECA, external carotid artery; EMS, encephalomyosynangiosis; FLAIR, fluid-attenuated inversion recovery; ICA, internal carotid artery; MMD, moyamoya disease; MMS, moyamoya syndrome; MRI, magnetic resonance imaging; PCA, posterior cerebral artery; PCD, protein C deficiency; P2, P2 portion of posterior cerebral artery; STA-MCA, superficial temporal artery-middle cerebral artery; SPECT, single photon emission computed tomography.

* Corresponding author. Tel.: +81 75 751 3459; fax: +81 75 752 9501.
E-mail address: kikuta@kuhp.kyoto-u.ac.jp (K. Kikuta).

0090-3019/$ – see front matter © 2005 Elsevier Inc. All rights reserved.
doi:10.1016/j.surneu.2004.04.027

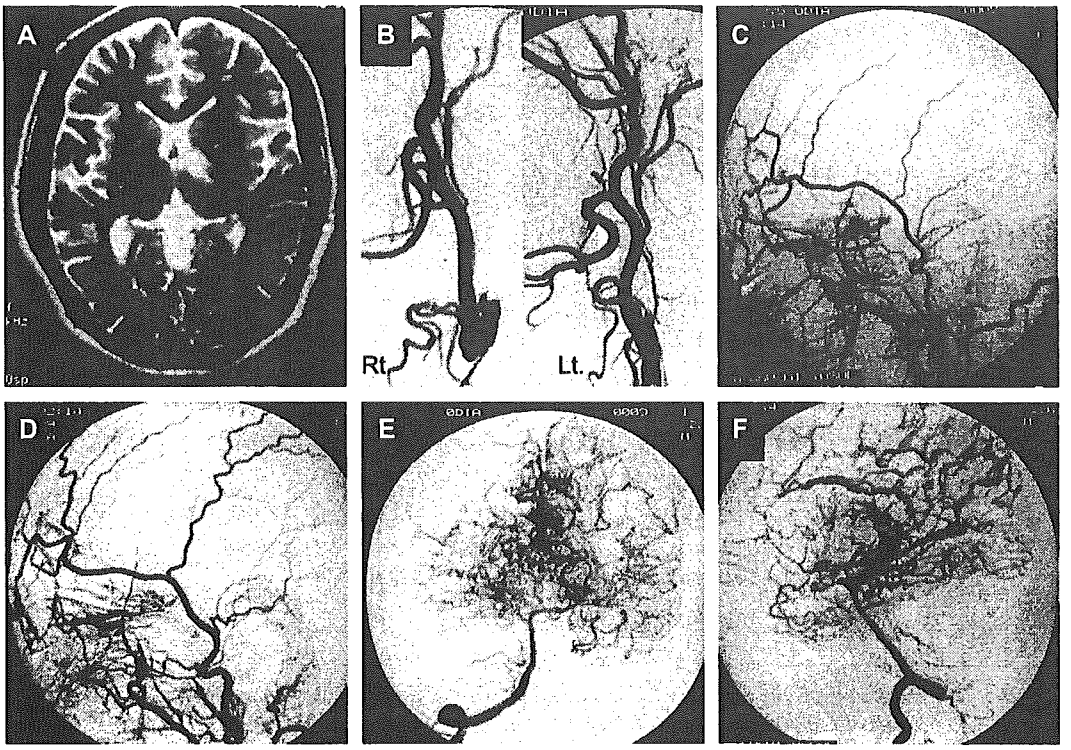

Fig. 1. A: Axial T2-weighted image of MRI demonstrating an ischemic lesion on the knee of the internal capsule. B: Bilateral carotid angiograms disclosed occlusion of ICAs at their origins. Right (C) and left (D) external angiogram (lateral view) demonstrating transdural anastomosis. Right vertebral angiogram (anteroposterior view, E; lateral view, F) showing extensive collateral circulation via leptomeningeal anastomosis around bilateral P2 portions.

not described on the angiography via the collateral circulation. Therefore, both ICAs were occluded entirely between the origin and the carotid fork. The patient had no underlying disease and the plasma protein C value was not examined at this time because MMS with PCD had not been reported yet. Although the angiographic findings were atypical according to the diagnostic criteria of MMD, her diagnosis was MMD because Suzuki and Takaku [15] had previously reported the similar angiographic findings in a patient with advanced MMD. The patient arrived at the neurosurgical clinic at Kyoto University Hospital on January 1, 1994. The magnetic resonance imaging (MRI) showed signal voids in the bilateral basal ganglia, infarction at the left knee of the internal capsule, and border zone infarction at the right parietal lobe (Fig. 1A). [^{123}I]-Single photon emission computed tomography revealed decreased cerebral blood flow in the bilateral cerebral hemisphere. She was treated surgically with right STA-MCA anastomosis with EMS on February 24 and with left STA-MCA anastomosis with EMS on March 24. Postoperative angiography showed extensive blood filling via ECAs and no abnormal findings were observed in the dural sinus (Fig. 2). Postoperatively, no ischemic attacks have occurred for 7 years.

On December 21, 2001, she suddenly developed left-sided hemiparesis and was admitted to our hospital. Upon

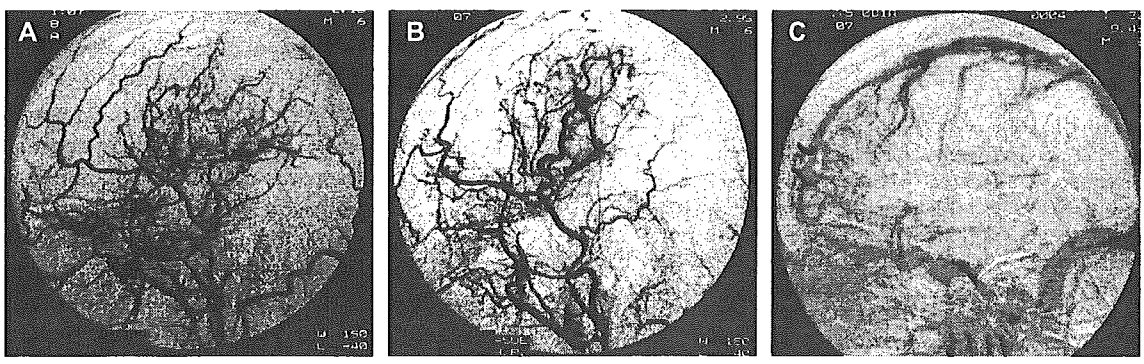

Fig. 2. Postoperative right (A) and left (B) external carotid angiograms (lateral view) demonstrating extensive blood supply via bilateral STA-MCA anastomose with EMS. C, Left external carotid angiogram (lateral view) showing intact dural sinus.

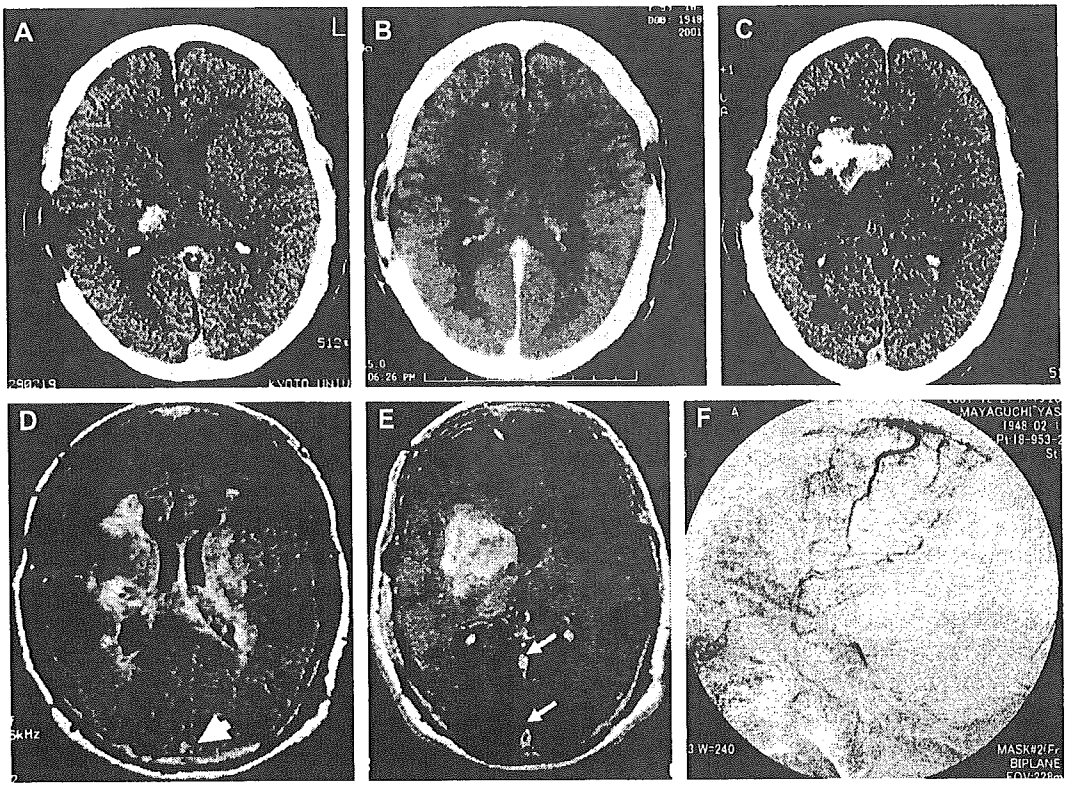

Fig. 3. Axial CT on December 21, 2001 (A), on December 27 (B), and on January 4, 2002 (C), demonstrating progression of intracerebral hemorrhages with peripheral edema. D: Axial fluid-attenuated inversion recovery image of MRI indicating thrombus within the superior sagittal sinus (arrowhead). E: Axial T1-weighted image with contrast enhancement showing filling defect of contrast medium within the superior sagittal sinus and the straight sinus (arrows). F: Left external carotid angiogram demonstrating sinus thrombosis including the superior sagittal sinus, the transverse sinus, and the straight sinus.

admission, brain CT demonstrated intracerebral hemorrhage in the right thalamus (Fig. 3A). It was initially believed that the hemorrhage was caused by the disruption of moyamoya vessels and she underwent medical treatment. However, her level of consciousness deteriorated to a state of comatose with repetitive partial seizures. A brain CT on December 27 revealed another lesion in the right basal ganglia including the caput nuclei caudati (Fig. 3B). The hematoma in the right basal ganglia was enlarged on the CT of January 4, 2002 (Fig. 3C). Magnetic resonance imaging on December 28 showed thrombus within the dural sinus (Fig. 3D, E). Angiographic study revealed patency of bilateral STA-MCA anastomosis, but the dural sinus including the superior sagittal sinus, the transverse sinus, and the straight sinus was occluded (Fig. 3F).

Laboratory investigations showed the following: Hematologic and chemical tests showed mild state of dehydration and hyperglycemia in the patients who were normalized soon after admission. Platelet counts, prothrombin time, activated partial thromboplasmin time, fibrinogen, and thrombin time were all within normal limits. Antinuclear antibodies and anti-cardiolipin antibodies were negative. The value of plasma protein C was reported as 48% and 55% on December 28 and January 25, 2002, respectively (normal, 64-146%). Although the patient was in a state of mild dehydration and hyperglycemia, these conditions could not affect the protein C value. The diagnosis of the patient was congenital PCD. According to radiologic and laboratory findings, the diagnosis of the patient was MMS associated with congenital PCD [13,14]. It was thought that dural sinus thrombosis was also caused by the underlying PCD. She was treated with systemic heparinization and with barbiturate coma therapy for 1 week. Her consciousness recovered to the level similar to that upon initial admission to the hospital but mild left-sided hemiparesis was residual. She was discharged and transferred to another hospital for further rehabilitation on February 20, 2002.

3. Discussion

According to the guidelines for MMD updated in 1997, the diagnosis of the patient is MMD when the steno-occlusive change around the carotid fork and the development of abnormal vascular network (moyamoya vessels) are observed bilaterally on the cerebral angiography without any underlying disease [4]. Similar angiographic findings were often observed in the patient with arteriosclerosis, autoimmune disease, meningitis, brain neoplasm, Down syndrome, Recklinghausen disease, head trauma, irradiation to the head, and others [4]. In addition, recent reports showing angiographic findings like MMD were also

Table 1
Cases of MMD or MMS with PCD previously reported

Case	Age	Sex	Onset	Surgical treatment	PCD	Dural sinus thrombosis	Another underlying diseases or conditions
Tsuda et al [16]	3	F	TIA	(−)	(+)	(−)	(−)
	13	F	TIA	STA-MCA	(+)	(−)	(−)
	3	M	TIA	(−)	(+)	(−)	Hereditary spherocytosis, protein S deficiency
	14	F	TIA	(−)	(+)	(−)	β-Thalassemia
Andeejani et al [1]	6	F	Stroke	(−)	(+)	(−)	(−)
Gururaj et al [6]	3	M	Stroke	(−)	(+)	(−)	Down syndrome
This case	54	F	Stroke	STA-MCA	(+)	(+)	(−)

observed in the patients with thalassemia, Fanconi anemia, liver transplantation, protein S deficiency, and PCD [3,7,16]. These patients are evaluated as having moya-moya-like disease, MMS, quasi-MMD, or akin MMD. In this paper, we use the term *MMS* to describe such patients [7,12]. Angiographic findings of our patient were atypical, but her diagnosis was MMD because bilateral occlusion of ICAs between their origin and the carotid fork with extensive development of collateral circulation via ECAs or PCAs could be taken as stage VI in the Suzuki and Takaku grade [15] of MMD. It has been previously reported that involvement of extracranial ICA, ECA, or vertebrobasilar systems can also be seen in some of the patients with MMD [8,11].

Protein C is a vitamin K-dependent plasma inhibitor protein which, once activated, acts as an anticoagulant during blood coagulation by impairing the coagulation factors, factors V and VIII [13,14]. Therefore, PCD is a risk factor of thrombosis especially in the venous system [13,14,18]. Because MMS with PCD had not been reported before 1993, the value of plasma protein C was not examined at the first admission [16]. At the second admission, the patient was in a state of mild dehydration and hyperglycemia but these conditions could not affect the protein C value [13]. Considering the mild degree in the decrease of plasma protein C value, the diagnosis of the patient was individual heterozygous with congenital PCD [2,13,14].

Thrombophobia in the patient with MMD or decrease of plasma protein C level in childhood cerebrovascular occlusive accidents have already been reported [10,16,17]. The patients with MMD with underlying PCD were first reported by Tsuda et al [16]. Among the 15 patients with MMD and the 4 patients with MMS in their series, PCD was observed in 2 patients with MMD and 2 patients with MMS. After their report, the patient with MMD associated with PCD has often been described as the patient with MMS [1,6] (Table 1). Andeejani et al [1] reported another case of a 6-year-old boy with MMS associated with PCD. Angiographic findings of this case were so unusual that steno-occlusive change involved bilateral extracranial ICAs, extracranial ECAs, and the basilar artery [1]. It is interesting that involvement of extracranial arteries was also observed in our case. These findings may often be observed in the patient with MMS associated with PCD. All 6 patients with MMS having PCD in the previous reports were pediatric cases (Table 1) [1,6,16]. This is the first report of an adult patient with MMS associated with PCD. Especially when the extracranial arteries are involved in the patients with MMD, MMS with PCD should be noted [1].

In our case, delayed dural sinus thrombosis occurred. It is quite rare that venous or dural sinus thrombosis is accompanied with MMD or MMS [5]. Only one pediatric case of MMS with Down syndrome has been reported to develop dural sinus thrombosis [5]. This case had no PCD. Our study is the first report of a patient with MMS with dural sinus thrombosis with underlying PCD. Protein C deficiency often causes venous thrombosis including dural sinus thrombosis [9,13,14]. Therefore, risk of sinus thrombosis should be taken into consideration in the treatment of MMS with PCD. Add in anticoagulation therapy to cerebral revascularization in the treatment for these patients is recommended.

4. Conclusion

An adult case of MMS that developed dural sinus thrombosis associated with PCD is reported. When the extracranial arteries are involved in the patients with MMD, MMS with PCD should be ruled out. In the treatment for the patient with MMS associated with PCD, anticoagulation therapy in addition to cerebral revascularization is recommended.

References

[1] Andeejani AMI, Salih MAM, Kolawole T, Grader TO, Damegh SAI, Boukai AAI. Moyamoya syndrome with unusual angiographic findings and protein C deficiency: review of the literature. J Neurol Sci 1998;159:11-6.

[2] Broekmans AW, Veltkamp JJ, Bertina RM. Congenital protein C deficiency and venous thromboembolism. A study of three Dutch families. N Engl J Med 1983;309:340-4.

[3] Deniz A, Sumer Y, Nesrin S, Belma A, Yavuz GYK. Moyamoya syndrome with protein S deficiency. Eur J Paediatr Neurol 2000;4: 185-8.

[4] Fukui M. Members of the research committee on spontaneous occlusion of the circle of Willis (Moyamoya disease) of the Ministry of Health and Welfare, Japan. Guidelines of the diagnosis and treatment of spontaneous occlusion of the circle of Willis (Moyamoya disease). Clin Neurol Neurosurg 1997;99(Suppl. 2): S238-40.

[5] Genoveva D-RC, Ana LO, Antonio P-H, Manuela CL, Imad A-A, Mercedes R-M. Moyamoya disease and sagittal sinus thrombosis in a child with Down's syndrome. Pediatr Radiol 2001;31:125-8.
[6] Gururaj A, Hardy D, Al-Gazali LI, Sztriha L, Roos A, Nork M. Are the strokes in moyamoya syndrome associated with Down syndrome due to protein C deficiency? Brain Dev 2002;24:719-22.
[7] Hoffman HJ. Moyamoya disease and syndrome. Clin Neurol Neurosurg 1997;99(Suppl. 2):S39-44.
[8] Houshimaru M, Kikuchi H. Involvement of the external carotid arteries in moyamoya disease: neuroradiological evaluation of 66 patients. Neurosurgery 1992;31:398-400.
[9] Kuwahara S, Abe T, Uga S, Mori K. Superior sagittal sinus and cerebral cortical venous thrombosis caused by congenital protein C deficiency: case report. Neurol Med Chir (Tokyo) 2000;40:645-9.
[10] Mariana B, Mirta H, Gabriela S, Aurora FT, Silvia T. Prothrombotic disorders in children with moyamoya disease. Stroke 2001;32:1786-92.
[11] Miyamoto S, Kikuchi H, Karasawa J, Nagata I, Ikota T, Takeuchi S. Study of the posterior circulation in moyamoya disease. J Neurosurg 1984;61:1032-7.
[12] Natori Y, Ikezaki K, Matsushima T, Fukui M. 'Angiographic moyamoya' it's definition, classification, and therapy. Clin Neurol Neurosurg 1997;99(Suppl. 2):S168-72.
[13] Robert IH. Disorders of coagulation and thrombosis. In: Braunwald E, Fauci AS, Kasper DL, Hauser SL, Longo DL, Jameson JL, editors. Harrison's principle of internal medicine. 15th ed. New York: McGraw Hill; 2001. p. 751-61.
[14] Serigsohn U, Lubetsky A. Genetic susceptibility to venous thrombosis. N Engl J Med 2001;16:1222-31.
[15] Suzuki J, Takaku A. Cerebrovascular "moyamoya" disease: disease showing abnormal net-like vessels in base of brain. Arch Neurol 1969;20:288-9.
[16] Tsuda H, Hattori S, Tanabe S, Nishioka S, Matsushima T, Ikezaki K, Fukui M, Kinoshita S, Hamashaki N. Thrombophilia found in patients with moyamoya disease. Clin Neurol Neurosurg 1997;99(Suppl. 2):S229-33.
[17] Uysal S, Anlar B, Atlay C, Kirazli S. Role of protein C in childhood cerebrovascular occlusive accidents. Eur J Pediatr 1989;149:216-8.
[18] Zunker P, Hohenstein C, Plendl H-J, Zeller JA, Caso V, Georgiadis A, Allardt A, Deushl G. Activated protein C resistance and acute ischemic stroke: relation to stroke causation and age. J Neurol 2001;248:701-4.

J Neurosurg 103:304–310, 2005

Survival and differentiation of neural progenitor cells derived from embryonic stem cells and transplanted into ischemic brain

YASUSHI TAKAGI, M.D., PH.D., MASAKI NISHIMURA, M.D., PH.D., ASUKA MORIZANE, M.D., PH.D., JUN TAKAHASHI, M.D., PH.D., KAZUHIKO NOZAKI, M.D., PH.D., JUNYA HAYASHI, M.D., AND NOBUO HASHIMOTO, M.D., PH.D.

Department of Neurosurgery, Graduate School of Medicine, Kyoto University, Kyoto, Japan

Object. Cell replacement therapy including the use of embryonic stem cells (ESCs) may represent a novel treatment for damage from stroke. In this study, the authors transplanted neural progenitor cells (NPCs) derived from ESCs into ischemic brain and analyzed their survival and differentiation.

Methods. Multipotential NPCs were generated from ESCs by using the stromal cell–derived inducing activity method. These cells could differentiate in vitro into neurons, glia, and oligodendrocytes, thus revealing them to be neural stem cells. The NPCs were then transplanted into ischemic brain. At 2 weeks postischemia, the transplanted cells occupied 18.8 ± 2.5% of the hemispheric area; by 4 weeks postischemia, 26.5 ± 4% of the hemisphere. At 4 weeks after transplantation, green fluorescent protein (GFP)–positive transplanted cells showed mature neuronal morphological features. The authors also investigated the expression of differentiation markers and various neurotransmitters. Transplanted cells were immunopositive for neuronal nuclei, β-tubulin-III, and glial fibrillary acidic protein. Of the GFP-positive cells, 33.3 ± 11.5% were positive for glutamate decarboxylase, 13.3 ± 5.8% for glutamate, 2.1 ± 2.5% for tyrosine hydroxylase, 1.8 ± 2% for serotonin, and 0.4 ± 0.2% for choline acetyltransferase.

Conclusions. The authors confirmed the survival and differentiation of ESC-derived NPCs transplanted into the ischemic brain. Surviving transplanted cells expressed several neural markers and neurotransmitters. These findings indicate that these cells can function in the brain.

KEY WORDS • **neural progenitor cell** • **embryonic stem cell** • **brain ischemia** • **stroke** • **mouse**

STROKE affects millions of people worldwide, with more than 500,000 new patients per year in the US alone. Although fewer than one third of strokes are fatal, approximately 60% of patients show significant residual impairments and the prevalence of stroke-related morbidity is expected to increase as the population ages because there is no therapy to reverse these effects. Cell replacement therapy, including the use of ESCs,[8] neural stem cells,[19,20,23,26,29] and bone marrow stromal cells,[3,6,7,15,16,32] may represent a novel treatment for stroke damage.[4,13]

Embryonic stem cells can be expanded to large numbers while maintaining their potential to differentiate into various somatic cell types of the three germ layers, and the in vitro differentiation of ESCs thus can provide donor cells for transplantation therapies. Indeed, ESCs have been found to differentiate in vitro into many clinically relevant cell types, including hematopoietic cells, cardiomyocytes, insulin-secreting cells, neurons, and glia.[4,13] Following transplantation into the central nervous system, ESC-derived neural precursors have been shown to integrate into host tissue and, in some cases, to promote functional improvement.[8] After brain ischemia, many types of cells are lost, including neurons, glia, and oligodendrocytes. It is hoped that NPCs can produce replacements.[26,31] Recently, Kawasaki and colleagues[12] reported that the SDIA method could easily produce NPCs from ESCs. In the present study, we generated NPCs from ESCs, expanded them as neurospheres, and transplanted them into the ischemic brain. To our knowledge, this is the first report on the use of ESC-derived neurons for transplantation into the ischemic brain.

Abbreviations used in this paper: ChAT = choline acetyltransferase; CNPase = cyclic nucleotide phosphodiesterase; ESC = embryonic stem cell; GAD = glutamate decarboxylase; GalC = galactocerebroside; GFAP = glial fibrillary acidic protein; GFP = green fluorescent protein; LIF = leukemia inhibitory factor; MCA = middle cerebral artery; NeuN = neuronal nuclei; NPC = neural progenitor cell; PBS = phosphate-buffered saline; rCBF = regional cerebral blood flow; SDIA = stromal cell–derived inducing activity; TH = tyrosine hydroxylase; TuJ1 = β-tubulin-III.

Materials and Methods

Induction of Neural Differentiation of ESCs

Undifferentiated murine ESCs (G4-2) were maintained on gelatin-coated dishes in Glasgow minimum essential medium (Sigma, St.

Louis, MO) supplemented with 1% fetal calf serum (JRH Biosciences, Tokyo, Japan), 5% KnockOut serum replacement (Invitrogen Corp., Carlsbad, CA), 2 mM glutamine (Sigma), 0.1 mM nonessential amino acids (Invitrogen Corp.), 1 mM pyruvate (Invitrogen Corp.), 0.1 mM 2-mercaptoethanol (Sigma), and 2000 U/ml LIF (Invitrogen Corp.). The G4-2 cells (a kind gift from Dr. Hitoshi Niwa, Osaka University) carry the blasticidin S–resistance selection marker gene driven by the Oct3/4 promoter (active under differentiated status) and the puromycin-resistance selection marker gene driven by the CAG promoter and were maintained in medium containing 20 g/ml blasticidin S (Invitrogen Corp.) and 1.5 g/ml puromycin (Carlbiochem, San Diego, CA) to eliminate differentiated cells. The neurons were induced from murine ESCs by SDIA, as previously described.[12,21] Briefly, ESCs were cocultured on PA6 stromal cells in Glasgow minimum essential medium supplemented with 5% KnockOut serum replacement, 2 mM glutamine, 0.1 mM nonessential amino acids, 1 mM pyruvate, and 0.1 mM 2-mercaptoethanol (differentiation medium). The ESC colonies that formed on PA6 monolayers during 12 days of culture were used for making NPCs and were isolated by incubation with papain for 5 minutes at room temperature (Papain Dissociation System; Worthington Biochemical Corp., Lakewood, NJ). Isolated colonies were cultured in neurobasal medium (Invitrogen Corp.) with B27 supplement (Invitrogen Corp.), 20 ng/ ml fibroblast growth factor 2 (Upstate Biotechnology, Waltham, MA), 20 ng/ml epidermal growth factor (R&D Systems, Minneapolis, MN), and 10 ng/ml LIF for 1 week. The NPCs derived from the ESCs were collected and used for transplantation.

Immunofluorescence Study

Single- and double-immunofluorescence studies were performed after permeabilization and blocking for nonspecific binding with 0.3% Triton X-100 (Sigma) and 10% normal donkey serum (Jackson Immunoresearch Laboratories, Inc., West Grove, PA), respectively. Primary rabbit anti-TH antibody (1:60; Chemicon, Temecula, CA), mouse anti-TuJ1 antibody (1:300; Convance Research Products, Richmond, CA), rabbit anti-GFAP antibody (1:1000; Chemicon), and anti-CNPase (1:200; Chemicon) were used at 4°C overnight; donkey Cy3-labeled secondary antibodies (Jackson Immunoresearch Laboratories, Inc.) or donkey fluorescein isothiocyanate–labeled secondary antibodies (Jackson Immunoresearch Laboratories, Inc.) were used at room temperature for 120 minutes. Green fluorescent protein, contained in the ESCs, was visualized by its own fluorescence. The percentage of immunopositive cells after papain treatment was evaluated using a laser confocal microscope (Fluoview FV300; Olympus Optical Co., Tokyo, Japan).

Induction of Focal Ischemia

The C57BL/6 mice (20–25 g) were anesthetized with 2% isoflurane and anesthesia was maintained with 1.5% isoflurane in 70% N_2O/30% O_2. Regional cerebral blood flow was measured as described using a laser Doppler flowmeter (Omegawave, Tokyo, Japan) equipped with a flexible skull probe. The tip of the probe was fixed using an adhesive agent and its accelerator (Aron Alpha; Toa, Tokyo, Japan) on the intact skull over the ischemic cortex (2 mm posterior and 6 mm lateral from bregma). Steady-state baseline values were recorded before MCA occlusion, and rCBF during and after occlusion was expressed as a percentage of the baseline values.[9,10,28] Rectal temperature was maintained between 36.5 and 37.5°C with a homeothermic blanket. Focal cerebral ischemia was induced by the intraluminal filament technique. The left MCA was occluded using a No. 8-0 nylon monofilament (Ethicon, Somerville, NJ) coated with a mixture of silicone resin (Xantopren; Bayer Dental, Osaka, Japan) and a hardener (Elastomer Activator; Bayer Dental). This coated filament was introduced into the internal carotid artery through the common carotid artery, up to the origin of the anterior cerebral artery via the internal carotid artery, to occlude the MCA and posterior communicating artery. The animals that demonstrated a more than 80% reduction in rCBF from baseline were included in this study. Thirty minutes after MCA occlusion, while the mice were kept at 37°C by using a blanket, the filament was withdrawn from the common carotid artery to allow reperfusion.[9,10,28]

Infarct Volume

The infarct volume was calculated by summing the volumes of each section directly by using the NIH image analyzing system (Dr. Wayne Rasband, National Institutes of Health, Bethesda, MD).[28] The data were statistically analyzed using the unpaired t-test.

Cell Transplantation

While in a state of deep pentobarbital anesthesia, the mice were placed in a stereotactic frame (Narishige, Tokyo, Japan) 2 days after ischemia/reperfusion. Each animal received a 2-μl injection (1 μl/ minute) of neurospheres derived from ESCs into the lesioned striatum (from the bregma: anterior −0.5, lateral +2.5, ventral +3, incisor bar 0) via a Hamilton microsyringe fitted with a 26-gauge blunt needle.

Immunohistochemical Analysis

Fourteen (four animals) or 28 days (four animals) after transplantation, animals were killed with pentobarbital and perfused transcardially with PBS, followed by 4% paraformaldehyde. The mouse brains were postfixed overnight and equilibrated in graded sucrose. Coronal 40-μm sections were cut serially on a freezing microtome and postfixed in 4% paraformaldehyde for 10 minutes. After several washes in 0.1 M PBS, the sections were incubated for 1 hour at room temperature with 10% normal goat serum (Vector Laboratories, Burlingame, CA) containing 0.3% Triton X-100 (Sigma). Immunohistochemical staining was performed at 4°C for 16 hours using antibodies against NeuN (1:200; Chemicon), TuJ1 (1:300; Convance Research Products), GFAP (1:1500; Chemicon), GalC (1:100; Chemicon), GAD (1:100, Sigma), glutamate (1:200; Chemicon), ChAT (1:100; Chemicon), TH (1:60; Chemicon), serotonin (1:2000; Chemicon), with 2% normal goat serum, 0.3% Triton X-100, and 0.1% NaN_3 in PBS used as the diluent. After three rinses in PBS, the sections were incubated for 1 hour at room temperature with Cy3-labeled (Jackson Immunoresearch Laboratories, Inc.) or fluorescein isothiocyanate–labeled secondary antibodies (Jackson Immunoresearch Laboratories, Inc.). In some experiments, sections were incubated with a Cy3-labeled NeuN monoclonal antibody (1:300; Chemicon) at 4°C overnight. Immunostained sections were evaluated with the aid of a confocal microscope. Grafted ESCs were detected by their green fluorescence. The area of immunopositive cells was quantified in every fourth section throughout the graft and its surroundings.

Results

Neural Progenitor Cells Generated From ESCs

The SDIA method was originally created for making dopaminergic neurons. With this method, ESCs are routinely maintained on gelatin-coated dishes (Fig. 1a). When cultured on a monolayer of PA6 cells, however, they differentiate into NPCs within 10 days and into dopaminergic neurons within 14 days. Thus, we cultured ESCs on PA6 cells for 10 days and made neurospheres consisting of NPCs. These cells were positive for neural cell adhesion molecule, which is a marker of neuroprogenitors (Fig. 1b). The ESC-derived NPCs formed round neurospheres cultured in the medium (Fig. 1c). These cells could differentiate in vitro into neurons (TuJ1-positive; Fig. 1d and e), glia (Fig. 1d and e), and oligodendrocytes (Fig. 1f), thus indicating them to be neural stem cells.

Physiological Data and Infarct Volume

All animals that underwent surgery demonstrated a more than 80% reduction in rCBF from baseline and were included in this study. The mean rCBFs during ischemia and after reperfusion were 8.5 ± 3.6 and 102.2 ± 18.4%, respectively (five–eight mice per group; preoperative CBF was set as

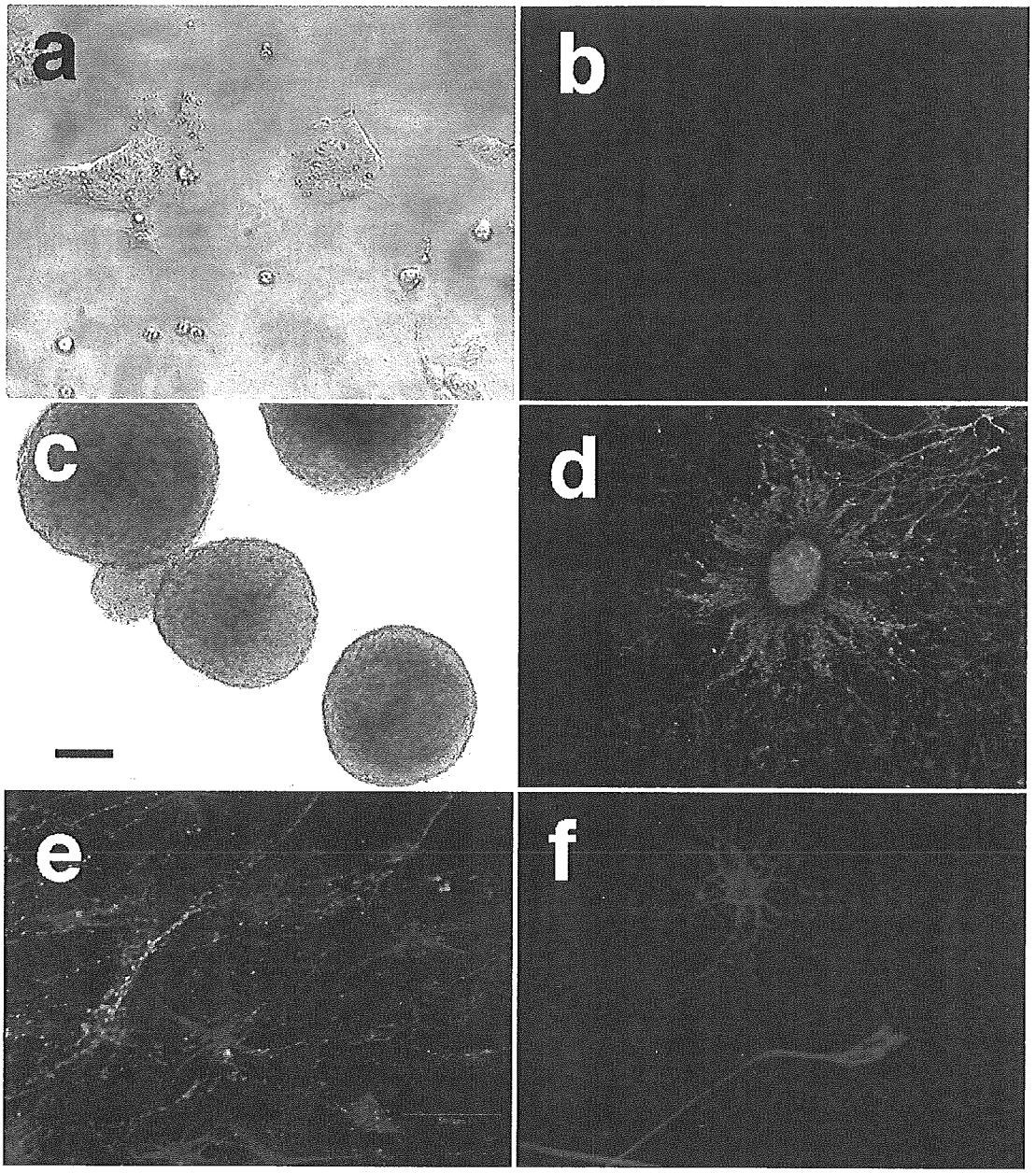

FIG. 1 a: Phase-contrast image of undifferentiated mouse ESCs cultured on a gelatin-coated dish. Fluorescence microscopy images of cells. b: Confoca microscope image of neural cell adhesion molecule expression (red) in differentiated mouse ESCs, which were cultured on PA6 cells for 10 days. c: Phase-contrast image of neurospheres derived from mouse ESCs. The differentiated ESCs become detached from the PA6 cell monolayer and form spheres. d and e: Confocal microscope images of differentiation from neurospheres derived from mouse ESCs. Neurospheres derived from ESCs were cultured on ornithine laminin–coated dishes for 7 days in the presence of LIF, fibroblast growth factor 2, and epidermal growth factor. Both TuJ1 (neuronal marker, green) and GFAP (glial marker, red) are expressed in neuroprogenitors differentiated from ESCs. f: Oligodendrocyte differentiation from neurospheres formed from ESCs. The CNPase (oligodendrocyte marker, red; TuJ1, blue) is expressed in differentiated neuroprogenitors. Original magnification × 40 (c), × 100 (a, b, and d), × 400 (e and f).

100%). Infarct volume at 2 and 4 weeks after transplantation was 9 ± 0.82 and 8.25 ± 1.26 mm, respectively (four mice per group). Note that the difference between the groups was not significant.

Transplantation of ESC-Derived NPCs Into Ischemic Brain

Thirty minutes of MCA occlusion resulted in brain infarction, which was restricted to the lateral striatum. Cells transplanted into the ischemic brain were located widely around the ischemic area (Fig. 2a–f). At 2 weeks after ischemia, the transplanted cells occupied 18.8 ± 2.5% of the hemispheric area (Fig. 2a–c and Table 1). By 4 weeks postischemia, this occupation increased to 26.5 ± 4% (Fig. 2d–f). On the contrary, in sham-operated animals, ESC-derived cells moved laterally along the corpus callosum. As

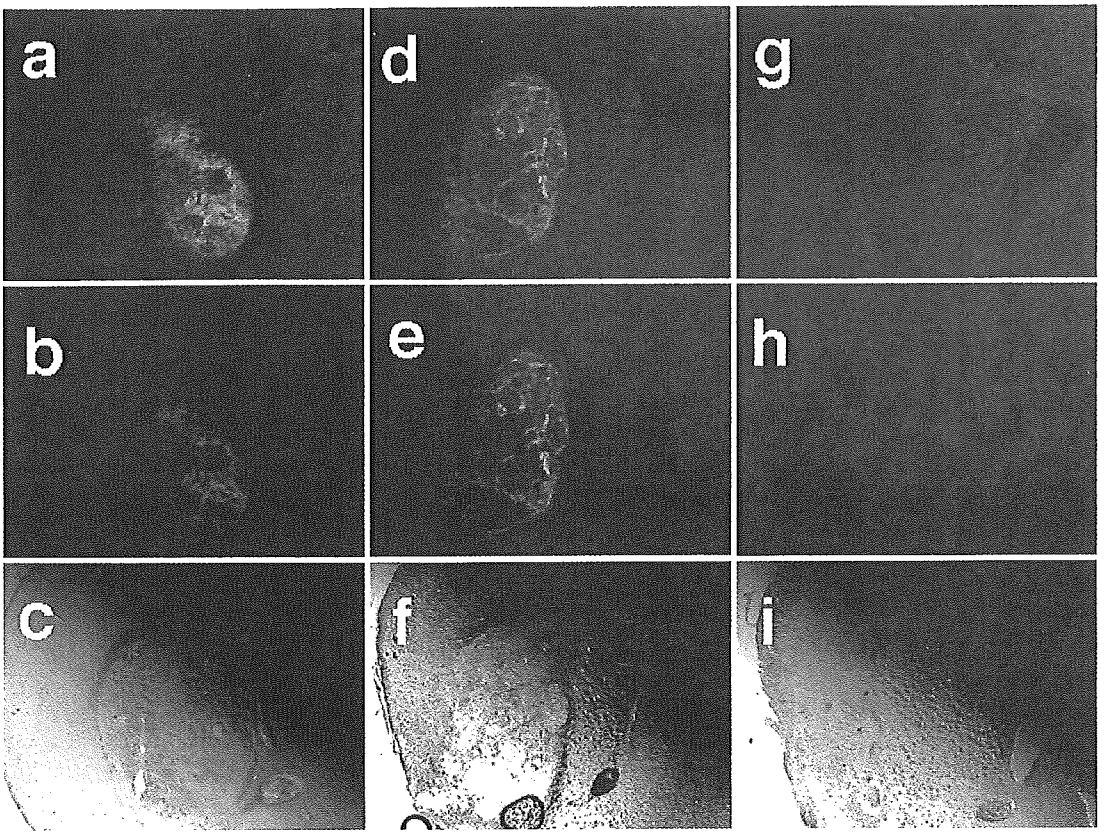

FIG. 2. Images demonstrating survival in the ischemic brain of transplanted neurospheres made from mouse ESCs 2 weeks after transplantation (a–c), 4 weeks after transplantation (d–f), and in sham controls (g–i). Red indicates NeuN (a, d, and g); green, GFP (b, e, and h). The GFP-positive cells occupied the ischemic areas (a–f), especially 4 weeks after ischemia (d–f). Interference differential microscopic images (c, f, and i) demonstrate the area of infarction, which was located in the lateral striatum after ischemia (c and f). Original magnification × 40.

shown in Fig. 2, surviving cells occupied a small area (Fig. 2g–i). Infarct volumes were not significantly different between the specimens prepared 2 weeks after ischemia and those 4 weeks after ischemia (data not shown).

Differentiation of Transplanted ESC-Derived NPCs

At 4 weeks after transplantation, GFP-positive cells demonstrated mature neuronal morphological features (Fig. 3a). In addition, we investigated the expression of both the differentiation markers and the various neurotransmitters (Fig. 3 and Table 2). Transplanted cells were immunopositive for NeuN (Fig. 3b), TuJ1, and GFAP (Fig. 3c). Of the GFP-positive cells, 60 ± 10% were NeuN-positive, 40 ± 10% TUJ1-positive, and 22 ± 7.2% GFAP-positive. Only 0.4 ± 0.5% of the GFP-positive cells were GalC-positive. Next we examined neurotransmitter expression of the transplanted cells. Of the GFP-positive cells, 33.3 ± 11.5% were GAD-positive (Fig. 3d), 13.3 ± 5.8% glutamate-positive (Fig. 3e), 2.1 ± 2.5% TH-positive (Fig. 3g), 1.8 ± 2% serotonin-positive (Fig. 3h), and 0.4 ± 0.2% ChAT-positive (Fig. 3e) cells.

TABLE 1

*Occupied area of transplanted cells in the brain**

Group	% of Hemisphere Occupied
controls	4.0 ± 1.2
2 weeks postischemia	18.8 ± 2.5
4 weeks postischemia	26.5 ± 4.0

* Data are expressed as the means ± standard deviation.

Discussion

In this study, we generated multipotential NPCs from ESCs and transplanted them into ischemic mouse brain. These cells could survive and expand widely in the ischemic area. Moreover, the transplanted NPCs differentiated into various types of neural cells.

TABLE 2

*Differentiation of transplanted cells in the ischemic brain**

Marker	% GFP
NeuN	60.0 ± 10.0
TuJ1	40.0 ± 10.0
GFAP	22.0 ± 7.2
GalC	0.38 ± 5.3
TH	0.6 ± 0.36
GAD	33.3 ± 11.5
Glutamate	13.3 ± 5.8
Serotonin	0.5 ± 0.44
ChAT	0.4 ± 0.2

* Data are expressed as the means ± standard deviation.

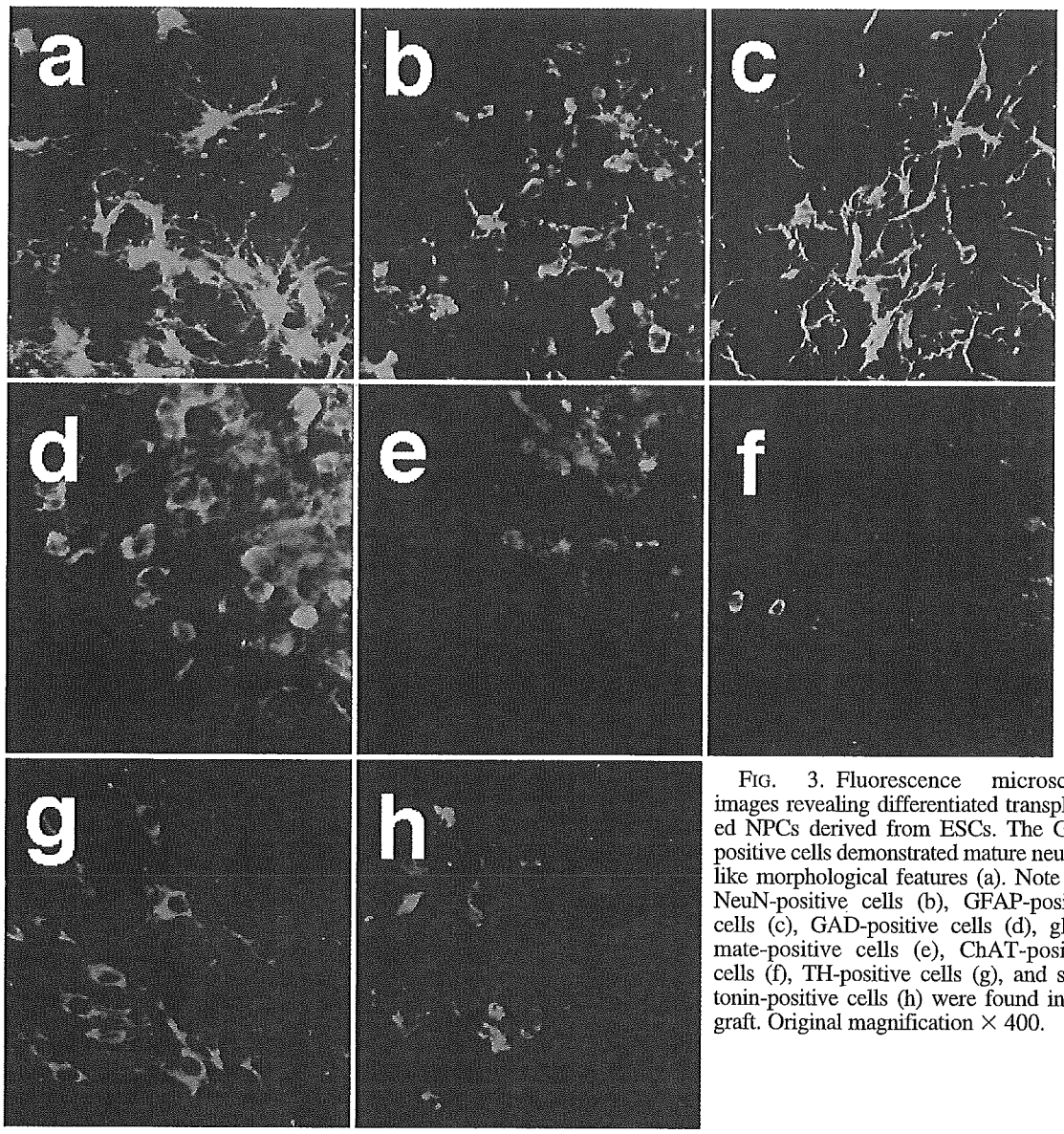

FIG. 3. Fluorescence microscopy images revealing differentiated transplanted NPCs derived from ESCs. The GFP-positive cells demonstrated mature neuron-like morphological features (a). Note that NeuN-positive cells (b), GFAP-positive cells (c), GAD-positive cells (d), glutamate-positive cells (e), ChAT-positive cells (f), TH-positive cells (g), and serotonin-positive cells (h) were found in the graft. Original magnification × 400.

Embryonic stem cells have many characteristics required for an optimal source for cell replacement therapy.[4] The ESCs are self-renewing, multipotent cells derived from the inner cell mass of the preimplantation blastocyst.[4] Kawasaki and colleagues[12] previously reported a strong neuralization-inducing activity present on the cell surface of stromal cells and named it "SDIA." In the absence of exogenous BMP4, mouse ESCs were shown to differentiate efficiently into NPCs and neurons when cultured on SDIA-possessing mouse stromal cells (PA6 cells) for 1 week.[12] Recently, the SDIA method has also become applicable for primate ESCs. After having been cultured on PA6 cells for 2 weeks, the majority of primate ESC colonies contained a large number of NPCs and postmitotic neurons.[12] Neural progenitor cells have multipotent, self-renewing capacities and can be cultured as neurospheres.

In this study, we analyzed several neurotransmitters' expressions. Note that GAD is a γ-aminobutyric acid synthetic enzyme. The γ-aminobutyric acidergic neurons in the cerebellum are rich in ventral mesencephalon or Purkinje cells. Choline acetyltransferase is a synthetic enzyme of acetylcholine. Cholinergic neurons are rich in the basal forebrain and associated with Alzheimer disease. Glutamate is used by descending pathways originating from neocortical pyramidal cells. The dorsal raphe nucleus is known to be rich in serotonin, which is implicated in emotion, fear, and cognition. Dopaminergic neurons of the substantia nigra are lost because of Parkinson disease. Tyrosine hydroxylase expression is linked to the secretion of levadopa, which is a dopamine precursor.[25,27,30] To determine cell types, we used several markers. Beta-Tubulin-III is expressed in postmitotic neunrons at an early stage of development. The NeuN is a nuclear protein that is a marker of a mature neuron. Both GalC and CNPase are thought to be mature oligodendrocyte markers. As an astrocyte marker, GFAP is detectable during fetal glial development.[2]

The use of neural transplantation for the treatment of neurological diseases first became a potential therapeutic modality in 1979 when Bjorklund and colleagues[5,13,24] demonstrated that implanting dopaminergic-containing neurons

into the rat striatum improved functional deficits induced by damage to the nigrostriatal pathway. Since then, advances in neural transplantation have moved from the animal model to the human model, with varying degrees of success.[11,19,20,23,29] In the animal models, authors examined a wide variety of disease states—from degenerative diseases to trauma and stroke—and the tissues used for transplantation—from fetal tissue to tumor lines to stem cells.[19,20,23,26,29] In some models, implants provide a source of neurotrophic factors.[6,7,15] Successes in animal models have led to transplant trials in the human population. Patient trials have been focused on transplantation for Parkinson disease, Huntington disease, spinal cord injury, and stroke.[4,13] As research in animal models progresses, transplant trials may be initiated for the treatment of multiple sclerosis, traumatic brain injury, cerebral palsy, amyotrophic lateral sclerosis, Alzheimer disease, and other disorders.[4,13,26]

In patients disabled by stroke, the concept of restoring function by transplanting human neuronal cells into the brain is a novel one. Data obtained from a rat model of transient focal cerebral ischemia demonstrated that transplantation of fetal tissue restored both behavioral and motor functions.[17,19,20,29] As for studies in humans, Kondziolka and colleagues[14,18] reported the results of a clinical trial using human neuronal cells. In examining 12 patients in this trial, their initial objective was to demonstrate the safety and feasibility of the neuronal cell implantation procedure. Among the treatment groups, mean National Institutes of Health Stroke Scale total scores decreased and mean European Stroke Scale total scores increased—both changes indicating improvement.[14,18] The transplanted cells were proposed to have improved neurological function through a number of different mechanisms, including provision of neurotrophic support, production of neurotransmitters, reestablishment of local interneuronal connections, cell differentiation and integration, and improvement of regional O_2 tension.

In the present study, we used ESC-derived NPCs for transplantation. The advantage in ESCs is that they can be expanded easily compared with neural stem cells. We also confirmed the differentiation of ESC-derived NPCs. During ischemia, various types of neurons as well as glial cells and oligodendrocytes are lost. The ESCs could supply these cells. Interestingly, in the sham-operated control brains, the transplanted cells occupied only a small area. On the contrary, in the ischemic brain, the transplanted cells spread throughout the ischemic lesion. This result indicates that the fate of the graft is dependent on the host environment. After ischemia, several cytokines and growth factors are known to be released. Today, the family of growth and trophic factors has been proposed to affect the survival and development of neuroprogenitor cells. Among them, LIF and ciliary neurotrophic factor in addition to more traditional growth factors, such as platelet-derived growth factor, are considered to be potent promoters of neuroprogenitor cell proliferation and their eventual differentiation.[1,22] Moreover, brain-derived neurotrophic factor, another member of the neurotrophin family (which includes nerve growth factor, neurotrophin-3, and neurotrophin-4/5), was shown to have great potency in modulating the growth and survival of dopaminergic cells and their precursors.[1,22] Glial-derived neurotrophic factor has similar or even enhanced trophic effects on dopaminergic neurons and their precursors.[1,22]

In using a 30-minute ischemia model, we did not examine behavioral improvement after transplantation, because such a model demonstrates only a slight behavioral deficit, thus making it difficult to assess behavior. Therefore we will use a longer period of ischemia in the next study and will examine network formation.

Conclusions

In summary, we confirmed the survival and differentiation of ESC-derived NPCs transplanted into the ischemic brain. We used the SDIA method on murine ESCs. Note that this method is also effective on primate and even human ESCs. Our findings indicated that ESC-derived NPCs can function in the brain.

References

1. Abe K: Therapeutic potential of neurotrophic factors and neural stem cells against ischemic brain injury. **J Cereb Blood Flow Metab 20:**1393–1408, 2000
2. Allers KA, Sharp T: Neurochemical and anatomical identification of fast- and slow-firing neurones in the rat dorsal raphe nucleus using juxtacellular labelling methods *in vivo*. **Neuroscience 122:** 193–204, 2003
3. Beck H, Voswinckel R, Wagner S, Ziegelhoeffer T, Heil M, Helisch A, et al: Participation of bone marrow-derived cells in long-term repair processes after experimental stroke. **J Cereb Blood Flow Metab 23:**709–717, 2003
4. Bjorklund A, Lindvall O: Cell replacement therapies for central nervous system disorders. **Nat Neurosci 3:**537–544, 2000
5. Bjorklund A, Stenevi U, Dunnett SB, Iversen SD: Functional reactivation of the deafferented neostriatum by nigral transplants. **Nature 289:**497–499, 1981
6. Chen J, Sanberg PR, Li Y, Wang L, Lu M, Willing AE, et al: Intravenous administration of human umbilical cord blood reduces behavioral deficits after stroke in rats. **Stroke 32:** 2682–2688, 2001
7. Chen J, Zhang ZG, Li Y, Wang L, Xu YX, Gautam SC, et al: Intravenous administration of human bone marrow stromal cells induces angiogenesis in the ischemic boundary zone after stroke in rats. **Circ Res 92:**692–699, 2003
8. Erdo F, Buhrle C, Blunk J, Hoehn M, Xia Y, Fleischmann B, et al: Host-dependent tumorigenesis of embryonic stem cell transplantation in experimental stroke. **J Cereb Blood Flow Metab 23:** 780–785, 2003
9. Hara H, Friedlander RM, Gagliardini V, Ayata C, Fink K, Huang Z, et al: Inhibition of interleukin 1β converting enzyme family proteases reduces ischemic and excitotoxic neuronal damage. **Proc Natl Acad Sci USA 94:**2007–2012, 1997
10. Hara H, Huang PL, Panahian N, Fishman MC, Moskowitz MA: Reduced brain edema and infarction volume in mice lacking the neuronal isoform of nitric oxide synthase after transient MCA occlusion. **J Cereb Blood Flow Metab 16:**605–611, 1996
11. Hoehn M, Kustermann E, Blunk J, Wiedermann D, Trapp T, Wecker S, et al: Monitoring of implanted stem cell migration in vivo: a highly resolved in vivo magnetic resonance imaging investigation of experimental stroke in rat. **Proc Natl Acad Sci USA 99:**16267–16272, 2002
12. Kawasaki H, Mizuseki K, Nishikawa S, Kaneko S, Kuwana Y, Nakanishi S, et al: Induction of midbrain dopaminergic neurons from ES cells by stromal cell-derived inducing activity. **Neuron 28:**31–40, 2000
13. Kondziolka D, Wechsler L, Achim C: Neural transplantation for stroke. **J Clin Neurosci 9:**225–230, 2002
14. Kondziolka D, Wechsler L, Goldstein S, Meltzer C, Thulborn KR,

Gebel J, et al: Transplantation of cultured human neuronal cells for patients with stroke. **Neurology 55:**565–569, 2000
15. Li Y, Chen J, Chen XG, Wang L, Gautam SC, Xu YX, et al: Human marrow stromal cell therapy for stroke in rat: neurotrophins and functional recovery. **Neurology 59:**514–523, 2002
16. Li Y, Chen J, Chopp M: Adult bone marrow transplantation after stroke in adult rats. **Cell Transplant 10:**31–40, 2001
17. Mattsson B, Sorensen JC, Zimmer J, Johansson BB: Neural grafting to experimental neocortical infarcts improves behavioral outcome and reduces thalamic atrophy in rats housed in enriched but not in standard environments. **Stroke 28:**1225–1232, 1997
18. Meltzer CC, Kondziolka D, Villemagne VL, Wechsler L, Goldstein S, Thulborn KR, et al: Serial [18F]fluorodeoxyglucose positron emission tomography after human neuronal implantation for stroke. **Neurosurgery 49:**586–592, 2001
19. Modo M, Rezaie P, Heuschling P, Patel S, Male DK, Hodges H: Transplantation of neural stem cells in a rat model of stroke: assessment of short-term graft survival and acute host immunological response. **Brain Res 958:**70–82, 2002
20. Modo M, Stroemer RP, Tang E, Patel S, Hodges H: Effects of implantation site of stem cell grafts on behavioral recovery from stroke damage. **Stroke 33:**2270–2278, 2002
21. Morizane A, Takahashi J, Takagi Y, Sasai Y, Hashimoto N: Optimal conditions for in vivo induction of dopaminergic neurons from embryonic stem cells through stromal cell-derived inducing activity. **J Neurosci Res 69:**934–939, 2002
22. Moskowitz MA, Lo EH: Neurogenesis and apoptotic cell death. **Stroke 34:**324–326, 2003
23. Nelson PT, Kondziolka D, Wechsler L, Goldstein S, Gebel J, DeCesare S, et al: Clonal human (hNT) neuron grafts for stroke therapy: neuropathology in a patient 27 months after implantation. **Am J Pathol 160:**1201–1206, 2002
24. Perlow MJ, Kumakura K, Guidotti A: Prolonged survival of bovine adrenal chromaffin cells in rat cerebral ventricles. **Proc Natl Acad Sci USA 77:**5278–5281, 1980
25. Safford KM, Safford SD, Gimble JM, Shetty AK, Rice HE: Charcterization of neural/glial differentiation of murine adipose-derived adult stromal cells. **Exp Neurol 187:**319–328, 2004
26. Savitz SI, Rosenbaum DM, Dinsmore JH, Wechsler LR, Caplan LR: Cell transplantation for stroke. **Ann Neurol 52:**266–275, 2002
27. Spenger C, Hyman C, Studer L, Egli M, Evtouchenko L, Jackson C, et al: Effect of BDNF on dopaminergic, serotonergic and GABAergic neurons in cultures of human fetal ventral mesencephalon. **Exp Neurol 133:**50–63, 1995
28. Takagi Y, Harada J, Chiarugi A, Moskowitz MA: STAT1 is activated in neurons after ischemia and contributes to ischemic brain injury. **J Cereb Blood Flow Metab 22:**1311–1318, 2002
29. Watson DJ, Longhi L, Lee EB, Fulp CT, Fujimoto S, Royo NC, et al: Genetically modified NT2N human neuronal cells mediate long-term gene expression as CNS grafts in vivo and improve functional cognitive outcome following experimental traumatic brain injury. **J Neuropathol Exp Neurol 62:**368–380, 2003
30. Yadid G, Sotnik-Barkai I, Tornatore C, Baker-Cairns B, Harvey-White J, Pentchev PG, et al: Neurochemical alterations in the cerebellum of a murine model of Niemann-Pick type C disease. **Brain Res 799:**250–256, 1998
31. Zhang ZG, Jiang Q, Zhang R, Zhang L, Wang L, Zhang L, et al: Magnetic resonance imaging and neurosphere therapy of stroke in rat. **Ann Neurol 53:**259–263, 2003
32. Zhao LR, Duan WM, Reyes M, Verfaillie CM, Low WC: Immunohistochemical identification of multipotent adult progenitor cells from human bone marrow after transplantation into the rat brain. **Brain Res Brain Res Protoc 11:**38–45, 2003

Manuscript received April 14, 2004.
Accepted in final form April 13, 2005.
This work was supported by a grant-in-aid for scientific research and special coordination funds for promoting science and technology from the Ministry of Education, Culture, Sports, Science, and Technology of the Japanese government.

Address reprint requests to: Yasushi Takagi, M.D., Ph.D., Department of Neurosurgery, Graduate School of Medicine, Kyoto University, 54 Kawahara-cho, Shogoin, Sakyo, Kyoto 606-8507, Japan. email: ytakagi@kuhp.kyoto-u.ac.jp.

Available online at www.sciencedirect.com

SCIENCE DIRECT

Surgical Neurology 64 (2005) 325–330

SURGICAL NEUROLOGY

www.surgicalneurology-online.com

Imaging

Magnetic resonance angiography evaluation of external carotid artery tributaries in moyamoya disease

Masaru Honda, MD[a,*], Naoki Kitagawa, MD[a], Keisuke Tsutsumi, MD[a], Minoru Morikawa, MD[b], Izumi Nagata, MD[a], Makio Kaminogo, MD[c]

Departments of [a]Neurosurgery and [b]Radiology, Nagasaki University School of Medicine, Nagasaki 852-8501, Japan
[c]Department of Neurosurgery, Sasebo General Hospital, Sasebo 857-8511, Japan

Received 8 November 2004; accepted 29 December 2004

Abstract

Background and Purpose: High-resolution magnetic resonance (MR) image has been introduced to diagnose and follow-up moyamoya disease and visualized moyamoya vessels and internal carotid artery stenosis. This study was performed to assess the utility of MR angiography (MRA) for the evaluation of anastomotic channels through the external carotid artery (ECA) in moyamoya disease patients.

Methods: Twenty patients with moyamoya disease were reviewed. The cortical anastomosis and superficial temporal artery (STA), middle meningeal artery, and deep temporal artery by MRA were evaluated and were compared with those by digital subtraction angiography if obtained. Fifteen patients (24 hemispheres) underwent bypass surgery, including encephaloduroarteriosynangiosis in 14 hemispheres and STA–middle cerebral artery anastomosis with encephalomyosinangiosis in 10 hemispheres. Five patients did not undergo any surgery.

Results: MRA could show these vessels and the patency of anastomosis formed by the surgery and also showed naturally formed anastomosis and ECA tributaries in the patients who did not undergo any surgery.

Conclusion: MRA provides useful information for follow-up evaluation on the development of the ECA system in moyamoya disease.

Keywords: External carotid artery; Magnetic resonance angiography; Moyamoya disease

1. Introduction

Magnetic resonance imaging and angiography (MRA) have been taking over digital subtraction angiography (DSA) in the diagnosis of and follow-up for moyamoya disease [1,2,5-8,10,12-14,16,17]. However, most MRA studies have focused on the severity of internal carotid artery stenosis or changes in moyamoya vessels, and have rarely mentioned the appearance of the ECA system contributing the formation of collateral circulation [5-7,13,16,17]. Preoperative development of the ECA system depends on the collateral pathway for the affected brain, and it sometimes works as collateral branches [3,4]. Therefore, evacuation of it is also important to estimating the affected brain condition.

After surgery, ECA system flow reflects the surgical effect directly, and the ECA evaluation is therefore important to understand its clinical condition. We have used MRA for the evaluation of the ECA system in moyamoya disease, especially for postoperative follow-up, and report here the usefulness of this technique.

2. Methods

2.1. Patients

A series of 20 cases (34 sides) of moyamoya disease were studied (Table 1). There were 10 males and 10 females

Abbreviations: DSA, digital subtraction angiography; DTA, deep temporal artery; ECA, external carotid artery; EDAS, encephaloduroarteriosynangiosis; MCA, middle cerebral artery; MIP, maximum intensity projection; MMA, middle meningeal artery; MRA, magnetic resonance angiography; STA, superficial temporal artery; TIA, transient ischemic attack.

* Corresponding author. Tel.: +81 95 849 7375; fax: +81 95 849 7378.
E-mail address: mhonda@net.nagasaki-u.ac.jp (M. Honda).

0090-3019/$ – see front matter © 2005 Elsevier Inc. All rights reserved.
doi:10.1016/j.surneu.2004.12.020

aged 1 to 46 (mean 20) years. First clinical symptoms were TIA (n = 8), stroke (n = 4), intracerebral hemorrhage (n = 2), subarachnoid hemorrhage (n = 1), convulsion (n = 4), and none (n = 1).

2.2. Surgical intervention

Encephaloduroarteriosynangiosis (EDAS) was performed on 9 patients (14 sides), followed up for 1.5 to 15 (mean 10.6) years. Superficial temporal artery–middle cerebral artery (STA-MCA) anastomosis with encephalomyosynangiosis occurred in 8 patients (10 sides), which included 2 patients who underwent STA-MCA anastomosis with encephalomyosynangiosis and EDAS on each side. Five patients who did not undergo surgery were followed up for 1 to 10.5 (mean 4.4) years (Table 1).

2.3. Imaging

MRA was performed with a 1.5-T whole-body MR unit (Signa Horizon; General Electric Medical Systems, Milwaukee, Wis) with a standard head coil. Three-dimensional time-of-flight MRA was obtained with the parameters of 33.3/3.1 milliseconds (repetition time/echo time), flip angle of 20°, and 1 signal acquired. Ramp pulse, multislab, zero-fill interpolation, and chemical shift fat suppression techniques were also used. The field of view was 160 mm with a matrix of 256 × 256 (160) and a section thickness of 0.7 mm after zero-fill interpolation. The other imaging parameters included 5 slabs. The thickness of all slabs was 134 mm. The thickness of 1 slab was 34 mm. There were 24 partitions in 1 slab and 6 overlapping slices, which gave 146 sections. The total acquisition time was 10 minutes 56 seconds. The multislab imaging volume was oriented axially to cover the circle of Willis and included the distribution of the MCA and posterior cerebral artery. After data acquisition was completed and each of the 146 sections was reconstructed, MRA in different view directions was obtained by means of a maximum intensity projection (MIP) algorithm. To interpret MRA, both the MIP and section images were reviewed. Our institution induced direct bypass surgery as a surgical first choice for moyamoya disease a year ago. Until then, EDAS had been performed. Therefore, patients who underwent EDAS were followed for long periods. Preoperative DSA was performed in all patients, and postoperative DSA was obtained in 6 patients. In patients who underwent STA-MCA surgery, preoperative MRA and DSA were performed within a week before surgery. First postoperative MRA was performed at 0 to 2 weeks after surgery. Second and further MRA was performed at every 2 to 12 months. Postoperative DSA was obtained in 4 patients treated by STA-MCA anastomosis at 4 to 10 months after surgery, and 4 patients treated by EDAS at 2 to 13 years after surgery.

Table 1
Summary of cases

Case no.	Age, sex	Symptom	Angiographic stage	Surgery
1	8, M	TIA	rt 2, lt 3	lt EDAS
2	9, F	Epilepsy	bilat 3	bilat EDAS
3	3, M	TIA	rt 3, lt 2	bilat EDAS
4	2, F	TIA	bilat 2	bilat EDAS
5	9, F	TIA	rt 3, lt 1	rt EDAS, lt STA-MCA (at 24 y old)
6	3, M	Stroke	rt 3, lt 2	rt EDAS
7	42, M	Stroke	bilat 3	bilat EDAS
8	38, M	Stroke	bilat 3	bilat EDAS
9	42, F	TIA	bilat 3	bilat STA-MCA
10	3, M	Stroke	bilat 3	rt STA-MCA, lt EDAS
11	21, M	Stroke	rt 1, lt 3	lt STA-MCA
12	46, F	Hemorrhage	bilat 4	lt STA-MCA
13	5, M	TIA	rt 3, lt2	rt STA-MCA
14	34, F	Stroke	bilat 3	bilat STA-MCA
15	33, M	TIA	bilat 3	bilat STA-MCA
16	3, F	TIA/hemorrhage	bilat 3	–
17	15, F	Convulsion	bilat 3	–
18	42, F	Stroke	rt 3, lt 2	–
19	40, M	None	bilat 4	–
20	20, F	Hemorrhage	bilat 2	–

F indicates female; M, male; lt, left; rt, right; bilat, bilateral.

Table 2
Comparison of ECA tributaries between DSA and MRA

DSA/MRA	STA	MMA	DTA	Anastomosis
STA-MCA (preop)	11/11	11/11	8/8	0
STA-MCA (postop)	7/7	7/7	7/7	7/7
EDAS	6/6	6/6	5/4	5/5
No operation	4/4	4/4	2/2	2/2

Preop indicates preoperative period; postop, postoperative period.

2.4. Image analysis

Suzuki's classification was used for staging [16]. STA, deep temporal artery (DTA), and MMA were examined in the evaluation of the development of the ECA system. Angiogenesis was evaluated as a newly developed vascular signal compared with preoperative MRA. These were checked by single radiologist without any clinical information.

3. Results

The obtained hemispheres were 17 patients (27 sides). In preoperative period, 8 of STA-MCA anastomosed cases with 12 hemispheres were analyzed, and after this surgery, 6 cases with 7 hemispheres were analyzed. Six of EDAS cases and 3 of nonoperated cases were also analyzed. The rest of 3 cases or 8 sides lacked DSA or MRA in their follow-up. Total obtained numbers of STA, DTA, and MMA on DSA was 28, 28, and 22, on the other hand, those on MRA was 28, 28, and 20 (Table 2). There was high compatibility of the visualization of these vessels in both MRA and DSA. In the cases that underwent surgery, the development of anastomotic channels and dilatation of ECA